Indium-Labeled Macrocyclic Conjugates of Naltrindole: High-Affinity Radioligands for In Vivo Studies of Peripheral δ Opioid Receptors

Romain A. Duval,[†,‡] Rachel L. Allmon,[†,‡] and John R. Lever*[,†,‡,§]

Departments of Radiology and the Radiopharmaceutical Sciences Institute, and Medical Pharmacology and Physiology, University of Missouri−Columbia, Columbia, Missouri 65212, and Research Service, Harry S. Truman Veterans Administration Medical Center, Columbia, Missouri 65201

Received January 1, 2007

We have identified a series of hydrophilic indium-labeled DOTA and DO3A conjugates of naltrindole (NTI) that are suited to in vivo studies of peripheral δ opioid receptors. Indium(III) complexes, linked to the indole nitrogen of NTI by six- to nine-atom spacers, display high affinities (0.1−0.2 nM) and excellent selectivities for binding to δ sites in vitro. The [^{111}In]-labeled complexes can be prepared in good isolated yields (∼65%) with high specific radioactivities (>3300 mCi/μmol). The spacers serve as pharmacokinetic modifiers, and log $D_{7.4}$ values range from −2.74 to −1.79. These radioligands exhibit a high level of specific binding (75−94%) to δ opioid receptors in mouse gut, heart, spleen, and pancreas in vivo. Uptakes of radioactivity are saturable by the non-radioactive complexes, inhibited by naltrexone, and blocked by NTI. Thus, these radiometal-labeled NTI analogues warrant further study by single-photon emission computed tomography.

Introduction

The development of selective radioligands for molecular imaging of the three classical types (μ, κ, and δ) of cerebral opioid receptors has been an active research arena for over two decades.[1] For instance, *N*1′-([^{11}C]methyl)naltrindole[2] (Figure 1) allows quantitative positron emission tomography (PET) studies of δ opioid receptors in the brain of healthy persons[3] and patient populations.[4] Naltrindole (NTI, **1**) was designed by Portoghese and colleagues using the message−address concept.[5] The benzene ring of the indole provides a δ "address" by mimicking Phe[4] of enkephalin, while the 4,5-epoxymorphinan skeleton provides a strong, general opioid binding "message." The pyrrole serves as a spacer where *N*1′-substitutions preserve δ opioid receptor affinity and selectivity. Accordingly, NTI has been a useful scaffold for the construction of additional radioligands (Figure 1). Those with δ affinities in the picomolar range include [^{18}F]fluoroethyl[6] and *p*-[^{18}F]fluorobenzyl[7] derivatives for PET, and an [^{123}I]iodoallyl[8] derivative for single-photon emission computed tomography (SPECT). Bulk tolerance at the indole nitrogen is high, and even *N*1′-benzylfluorescein congeners display appreciable δ opioid receptor affinities (K_is 12−24 nM) and modest selectivities (4- to 40-fold) over μ and κ sites in vitro.[9]

Most radioligands for in vivo studies of opioid receptors have been designed for brain imaging and are lipophilic to permit passage across the blood−brain barrier.[1,10] However, there is an increasing need for in vivo imaging studies of peripheral opioid receptors to help assess the roles they may play in cancer,[11] cardiovascular disease,[12] gastrointestinal disorders,[13] and newer paradigms for pain relief that use peripherally restricted opioids.[14] The feasibility of imaging δ opioid receptors of normal human heart,[15] and δ sites overexpressed by the primary tumors of lung[16] and breast[17] cancer patients, has been demonstrated in limited studies using *N*1′-([^{11}C]methyl)naltrindole and PET. Hydrophilic opioid radioligands, designed for peripheral studies, might show lower nonspecific uptake, higher specific binding, faster blood clearance, and favorable radiation dosimetry. Further, a focus on hydrophilic ligands permits the use of chelated radiometals as the marker elements. Depending upon nuclear properties,[18] radiometal-labeled opioids might be employed for SPECT (e.g., ^{99m}Tc, ^{111}In) or PET (e.g., ^{68}Ga, ^{64}Cu) imaging or perhaps for radiotherapy (e.g., ^{90}Y, ^{177}Lu).

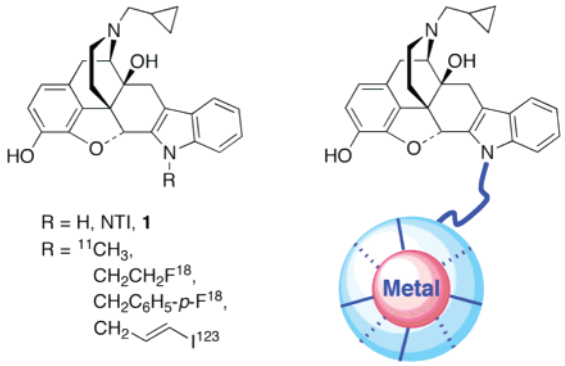

Figure 1. Structures of NTI, radiolabeled analogues, and a hypothetical radiometal-labeled *N*1′-conjugate.

The development of radiometal-labeled conjugates of small molecules that target receptors is a challenge for reasons including the large size of the metal coordination sphere with respect to the pharmacophore (cf. Figure 1), and considerations of the thermodynamic and kinetic stability of the chelated metal.[18,19] The polyaminocarboxylates DOTA[a] and DO3A are versatile chelators that form a variety of stable radiometal

* To whom correspondence should be addressed. Phone: (573) 814-6000 ext. 53686. Fax: (573) 814-6551. E-mail: leverj@health.missouri.edu.
† Department of Radiology and the Radiopharmaceutical Sciences Institute, University of Missouri−Columbia.
‡ Harry S. Truman Veterans Administration Medical Center.
§ Department of Medical Pharmacology and Physiology, University of Missouri−Columbia.

[a] Abbreviations: DOTA, 1,4,7,10-tetraazacyclododecane-1,4,7,10-tetraacetic acid; DO3A, 1,4,7,10-tetraazacyclododecane-1,4,7-triacetic acid; EDTA, ethylenediaminetetraacetic acid; DIBAL-H, diisobutylaluminum hydride; NTI, naltrindole; DAMGO, [D-Ala^2, *N*-MePhe^4, Gly^5-ol]enkephalin; DPDPE, [D-Pen^2, D-Pen^5]enkephalin; TIPP(ψ), H-Tyr-Tic[CH_2NH]-Phe-Phe-OH, Tic = 1,2,3,4-tetrahydroisoquinoline; U69,593, (+)-(5α,7α,8β)-*N*-methyl-*N*-[7-(pyrrolidin-1-yl)-1-oxaspiro[4,5]dec-8-yl] benzeneacetamide.

10.1021/jm0700013 CCC: $37.00
Published on Web 04/03/2007

Scheme 1[a]

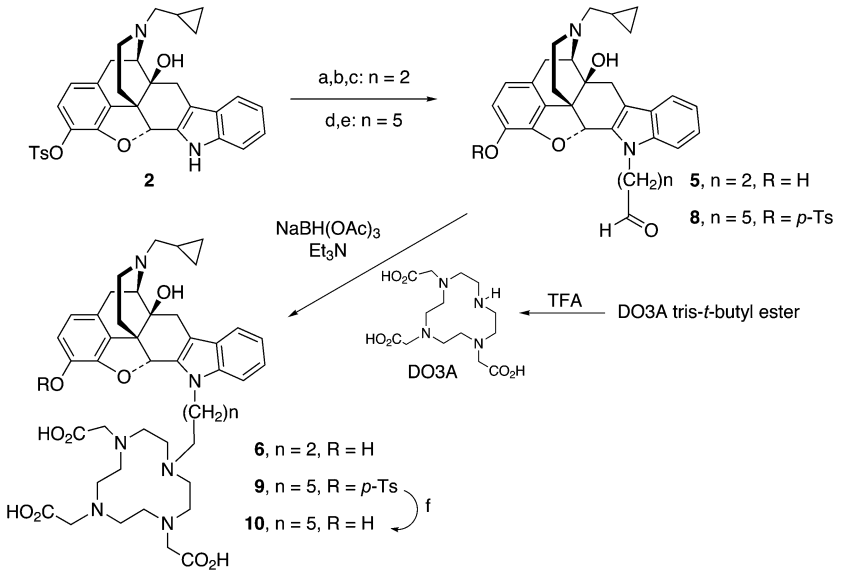

[a] Reagents and conditions: (a) 3-bromopropionaldehyde dimethylacetal, NaH, DMF, 2 h, 77%; (b) NaOH, *i*-PrOH, reflux, 15 h, 83%; (c) *p*-TsOH, acetone, 3 h, 74%; (d) 6-bromohexanenitrile, NaH, DMF, 1 h, 96%; (e) DIBAL-H, CH_2Cl_2, toluene, 15 min, 40%; (f) NaOH (1.0 N), reflux, 16 h, 64%.

complexes.[18,19] They are often used with indium-111, a radionuclide that has appropriate half-life (2.8 days) and γ-emission characteristics (171 and 245 keV) for SPECT imaging. These favorable properties, coupled with the acceptance of bulk at the indole nitrogen, prompted us to investigate a series of indium-(III) and [^{111}In]-labeled DOTA and DO3A conjugates of NTI. Here we report their synthesis, lipophilicities, and opioid receptor binding properties in vitro, along with data showing high levels of specific binding in vivo to the peripheral δ opioid receptors of mice.[20]

Results and Discussion

Organic Synthesis. Two approaches were employed for connecting NTI to DO3A or DOTA. In the first, conjugates were prepared by reductive amination of *N*1′-aldehyde derivatives with DO3A to afford three- and six-carbon alkyl linkers (Scheme 1). NTI, with the phenol protected by a tosyl moiety (**2**),[6a] was selectively alkylated at the indole nitrogen with 3-bromopropionaldehyde dimethylacetal to give **3** (77%), or with 6-bromohexanenitrile to give **7** (96%). Excess alkylating agent was required for good conversion due to competing β-elimination. Hydrolysis of **3** with warm base afforded **4** (83%), and the dimethylacetal protecting group was removed by acid-catalyzed transacetalization to give *N*1′-propionaldehyde **5** (74%). The complementary *N*1′-hexanaldehyde **8** was prepared in moderate yield (40%) by partial nitrile reduction of **7** using diisobutylaluminum hydride (DIBAL-H). These intermediates were coupled with DO3A, liberated from the tris(*t*-butyl ester) by neat trifluoroacetic acid (TFA),[21] using reductive amination mediated by $NaBH(OAc)_3$ and Et_3N to provide **6** (68%) and **9** (87%). With this selective borohydride reagent,[22] no alcohol was detectable from aldehyde reduction. Hydrolysis of **9** produced phenol **10** (64%) to complete the sequence.

In the second approach, *N*1′-aminoalkyl derivatives of NTI were coupled with the activated *N*-hydroxysuccinimidyl ester of DOTA (DOTA-NHS) to afford conjugates linked by six- and nine-atom alkylcarboxamide chains (Scheme 2). Alkylation of **2** with *N*-(3-bromopropyl)phthalimide gave **11** in good yield (84%). Hydrolysis of both protecting groups was accomplished in one step to give *N*1′-aminopropyl derivative **12** (93%). Treatment of *N*1′-hexanenitrile **7**, a common intermediate from the first approach, with methanolic *n*-Bu_4NOH provided phenol **13** (68%). Complete nitrile reduction using excess DIBAL-H gave *N*1′-aminohexyl derivative **14** (64%). Amines **12** and **14** were coupled with DOTA-NHS using Et_3N and catalytic 4-*N*,*N*′-dimethylaminopyridine (DMAP) to furnish a good yield of **15** (74%) and a modest yield of **16** (34%) as the TFA salts.

Scheme 2[a]

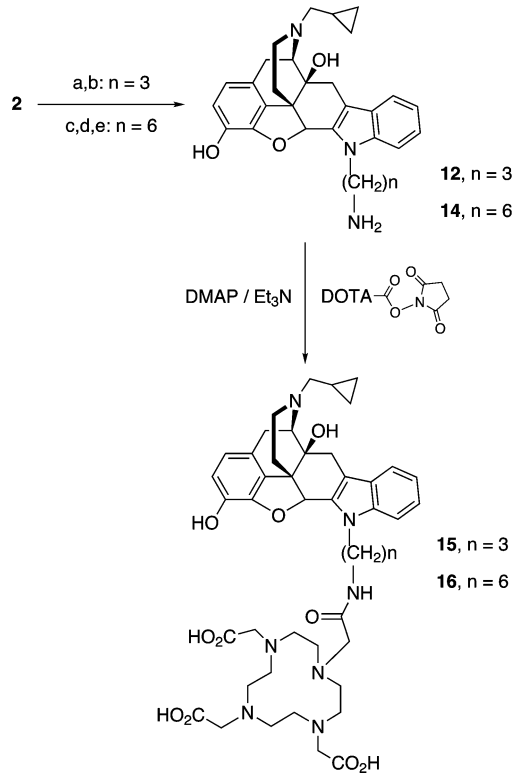

[a] Reagents and conditions: (a) *N*-(3-bromopropyl)phthalimide, NaH, DMF, 2 h, 84%; (b) NaOH, *i*-PrOH, reflux, 15 h, 93%; (c) 6-bromohexanenitrile, NaH, DMF, 1 h, 96%; (d) *n*-Bu_4NOH, CH_3OH, 1,4-dioxane, reflux, 8 h, 68%; (e) DIBAL-H, CH_2Cl_2, toluene, 3 h, 64%.

Complex Formation and Radiolabeling. Preparation of the non-radioactive and radioactive indium complexes proved straightforward (Scheme 3). Treatment of the DO3A (**6**, **10**)

Scheme 3. Preparation of Indium(III) and [^{111}In]-Labeled Complexes

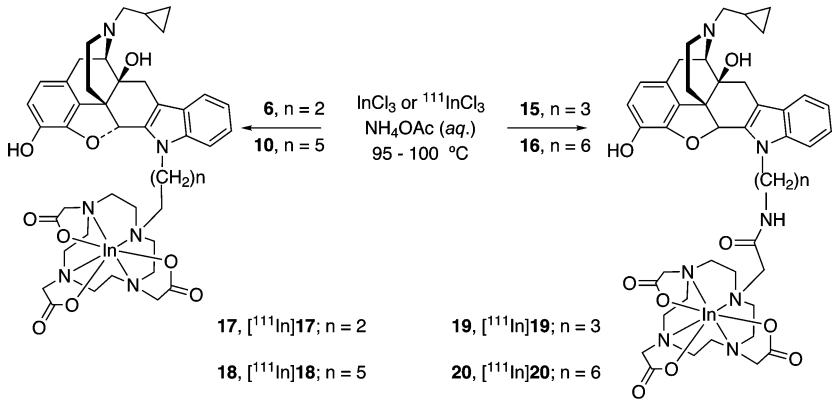

and DOTA (**15**, **16**) conjugates with $InCl_3$ at 100 °C for 30−45 min, followed by reversed-phase C18 chromatography and lyophilization, provided good isolated yields (69−95%) of **17**−**20** as TFA salts. The structures depicted in Scheme 3 represent the typical[18] seven-coordinate In^{3+} complexes shown by NMR spectroscopy to predominate in solution.[23] In the solid state, however, crystallographic data indicate that the carboxamide oxygen of DOTA complexes like **19** and **20** can participate in bonding, leading to an eight-coordinate, inverted square antiprism geometry.[23]

Similarly, treatment of the polydentate chelators with no-carrier-added [^{111}In]Cl_3 (0.5−3.8 mCi) in NH_4OAc buffer at 95−100 °C for 30 min gave 83−93% incorporations of radioactivity. Reversed-phase HPLC purification, followed by solid-phase extraction, provided good isolated yields (55−83%) of [^{111}In]**17**−[^{111}In]**20**. Average yields, over multiple preparations, were about 65%. All radioligands were obtained with high chemical and radiochemical purities, and coeluted with their non-radioactive counterparts under HPLC conditions that fully resolved the precursors from the complexes. Representative analytical traces are shown in Figure 2. Specific radioactivities exceeded 3300 mCi/μmol, and the radioligands were stable during overnight storage.

Lipophilicity. Relative lipophilicity is a key physicochemical parameter that influences pharmacokinetics.[10,24,25] Distribution coefficients were determined for [^{3}H]NTI and for complexes [^{111}In]**17**−[^{111}In]**20**, using *n*-octanol and pH 7.4 phosphate buffer (Table 1). For the DO3A (**6**, **10**) and DOTA (**15**, **16**) chelating agents, log P_{ow} values were calculated using ClogP software. All of the macrocyclic analogues of NTI were quite hydrophilic, and measured log $D_{7.4}$ values for the [^{111}In]complexes were negative. Differences noted between radiolabeled complexes were consistent with substituent constant additivity,[24] with the most lipophilic complex [^{111}In]**18** having a *n*-hexyl linker, and the most hydrophilic complex [^{111}In]**19** having an acetamidopropyl linker. Calculated log P_{ow} values for the parent DO3A and DOTA chelators showed Spearman rank order ($r = 0.98$, $p = 0.02$) correlation with log $D_{7.4}$ values measured directly for the radiolabeled complexes, but they were 1.1 to 1.8 log units higher due to computational treatment as neutral entities.

Competition Binding Assays. Opioid receptor binding assays (Table 1) were performed using membranes from fresh CD1 mouse (δ, [^{3}H]NTI)[26] or frozen guinea pig (μ, [^{3}H]DAMGO; κ, [^{3}H]U69,593) brains.[27] Although guinea pig brain has a significant population of δ sites,[6b,27] we chose to use mouse brain for these primary site assays because δ receptors, and their interactions with [^{3}H]NTI, are well defined in this tissue.[26a] Thus, the data represents binding of the novel ligands in vitro in one of the few tissues where δ opioid receptors have been characterized from the species to be used for in vivo studies

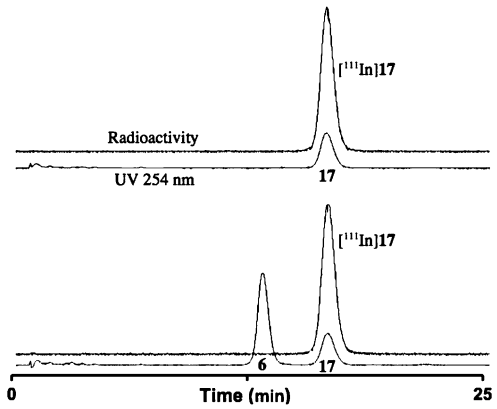

Figure 2. Reversed-phase HPLC chromatograms showing coelution of purified [^{111}In]**17** with a standard sample of **17** (top panel) and degree of separation between these complexes and precursor **6** (bottom panel).

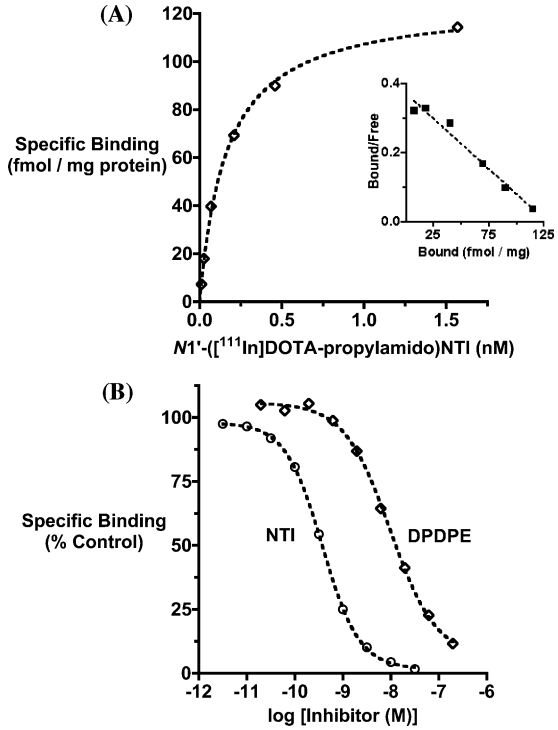

Figure 3. Panel A: Saturation binding isotherm, Rosenthal plot insert, for *N*1′-([^{111}In]DOTA-propylamido)NTI ([^{111}In]**19**) in mouse brain homogenates. Panel B: Inhibition of [^{111}In]**19** (0.15 nM, 1500 mCi/μmol) binding by δ receptor ligands.

Table 1. Opioid Receptor Binding Properties and Lipophilicity Measures for NTI, Its DOTA and DO3A Conjugates, and Their Indium Complexes

	K_i (nM)[a]			selectivity[b]		
compd	δ	μ	κ	μ/δ	κ/δ	log $D_{7.4}$[c] or ClogP[d]
1 (NTI)	0.15 ± 0.02	33.9 ± 0.76	14.9 ± 0.75	226	99	2.41 ± 0.08[c]
6	4.9 ± 0.31	1748 ± 248	2010 ± 268	357	410	−1.20[d]
17	9.7 ± 0.82	230 ± 24	1259 ± 175	24	130	−2.47 ± 0.011[c]
10	0.20 ± 0.01	48.2 ± 9.0	26.2 ± 2.8	241	131	0.038[d]
18	0.11 ± 0.01	34.4 ± 1.4	14.4 ± 1.0	313	131	−1.79 ± 0.010[c]
15	0.46 ± 0.03	130 ± 25	367 ± 74	283	798	−1.65[d]
19	0.21 ± 0.03	67.5 ± 6.0	510 ± 143	321	2428	−2.74 ± 0.012[c]
16	0.18 ± 0.01	96.6 ± 9.8	674 ± 28	537	3744	−0.64[d]
20	0.19 ± 0.01	35.3 ± 7.5	130 ± 12	186	684	−1.97 ± 0.004[c]

[a] Means ± SEM, $n = 3-6$. δ, [^{3}H]NTI, mouse brain; μ, [^{3}H]DAMGO, guinea pig brain; κ, [^{3}H]U69,593, guinea pig brain. Hill coefficients near unity (0.80−1.24). [b] K_i ratios. [c] Measured values ± SD, $n = 4$, for [^{3}H]NTI and [^{111}In]**17**−[^{111}In]**20** using *n*-octanol and pH 7.4 phosphate buffer. [d] Calculated using ClogP software.

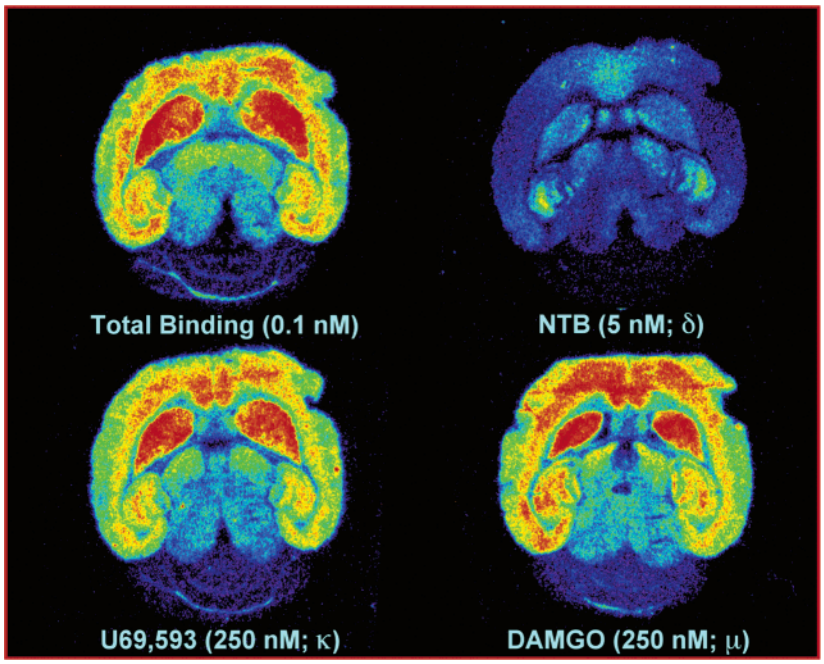

Figure 4. Pseudocolor images from in vitro autoradiography of δ sites in horizontal sections of mouse brain using *N*1′-([^{111}In]DOTA-propylamido)-NTI ([^{111}In]**19**) at 0.1 nM (1500 mCi/μmol) in the presence and absence of opioid receptor ligands naltriben (NTB), DAMGO, and U69,593.

(vide infra). The overall opioid receptor binding profile obtained for NTI agreed well with determinations by others using similar radioligands and tissues.[6b,26,28] The major finding for the novel compounds is the use of linkers having six to nine atoms preserves the high δ opioid receptor affinity of NTI and maintains or improves δ selectivity. These chelators (**10**, **15**, **16**) and their indium(III) complexes (**18**, **19**, **20**) give picomolar apparent affinities (K_is) for δ opioid receptors accompanied by >100-fold selectivities against secondary interactions at μ and κ sites. By contrast, **6** and **17** having three-atom linkers are far less potent binders at all opioid receptors. Nonetheless, their δ affinities are in the low nanomolar range, and δ selectivities are good. Examination of molecular models suggests that the shorter linker allows closer approach of the pendant moiety to the phenol. This would hinder binding to all opioid receptor types since the phenol contributes to the general binding message of 4,5-epoxymorphinans[29] through hydrogen bonding with histidine residue 17 of transmembrane domain (TM) VI.[30a] As a spot check for other interactions, NTI and the novel macrocyclic analogues were tested in σ_1 and σ_2 receptor binding assays,[31] and they showed no displacement of radioligand binding at 10 μM concentrations (data not shown).

The δ receptor affinities between pairs of polydentate chelators and their indium complexes (i.e., **6**/**17**; **10**/**18**; **15**/**19**; **16**/**20**) were similar, consistent with a lack of significant interactions with the hydrophobic address locus of the δ opioid receptor at TMs VI and VII.[27,30] However, the chelators generally exhibited lower affinities than the metal complexes for μ and κ sites. This signifies that structural features of the pendant macrocycle do influence these interactions, with free charged carboxylate groups detrimental to binding. Complexes **18** and **19** each have six-atom linkers, but they differ by design in the *n*-hexyl vs acetamidopropyl chains. Complex **18** was more potent than **19** for all three opioid receptors, but with lower δ over κ selectivity. The same trends were noted for the respective chelators **10** and **15**, indicating an effect of linker on binding. Together, the data show that subtle structural influences are felt some distance from the primary NTI pharmacophore. Interestingly, affinities tended to become higher with increasing lipophilicity for complexes **18**−**20**, with the most prominent effect at κ receptors (Table 1). The profile of **18**, having the highest lipophilicity, most closely resembled that of NTI. One might speculate that more lipophilic ligands present a greater effective concentration to the receptors by differential sequestration in membrane fragments.[32] This could enhance competition

Table 2. Biodistribution of [^{111}In]-Labeled Complexes **19** (log $D_{7.4}$ − 2.74), **20** (log $D_{7.4}$ − 1.97), and **18** (log $D_{7.4}$ − 1.79) in Male CD1 Mice[a]

[^{111}In]**19**

tissue	5 min	15 min	30 min	60 min	120 min	240 min
blood	3.40 ± 0.22	1.19 ± 0.10	0.58 ± 0.07	0.32 ± 0.10	0.32 ± 0.20	0.43 ± 0.35
heart	3.58 ± 0.28	4.01 ± 0.60	4.61 ± 0.64	3.65 ± 1.92	3.70 ± 0.29	2.46 ± 0.23
lung	2.79 ± 0.10	2.11 ± 1.23	1.08 ± 0.07	0.82 ± 0.18	0.71 ± 0.14	0.52 ± 0.10
liver	9.73 ± 2.49	20.96 ± 1.92	18.27 ± 2.42	13.08 ± 2.27	8.03 ± 1.52	4.40 ± 0.98
spleen	2.00 ± 0.18	2.30 ± 0.30	1.89 ± 0.72	2.34 ± 0.20	1.75 ± 0.16	1.36 ± 1.21
pancreas	1.48 ± 0.23	1.45 ± 0.31	1.84 ± 0.52	1.46 ± 0.81	1.67 ± 0.13	1.25 ± 0.47
stomach	1.52 ± 0.48	2.03 ± 0.38	3.65 ± 0.22	3.24 ± 1.81	5.08 ± 1.39	4.72 ± 3.08
s. intestine	3.06 ± 0.36	6.09 ± 0.69	9.45 ± 1.92	10.73 ±2.25	13.21 ±3.24	8.87 ± 2.40
cecum	1.01 ± 0.19	1.72 ± 0.22	1.74 ± 0.50	1.77 ± 0.20	5.55 ± 2.66	28.31 ± 14.18
l. intestine	1.94 ± 0.21	3.67 ± 0.84	3.58 ± 1.48	3.32 ± 0.40	5.31 ± 2.08	12.33 ± 3.52
kidney	6.82 ± 0.81	3.30 ± 1.34	1.55 ± 0.20	1.75 ± 0.42	1.61 ± 0.39	1.12 ± 0.01
muscle	0.78 ± 0.10	0.33 ± 0.03	0.19 ± 0.01	0.16 ± 0.02	0.12 ± 0.03	0.08 ± 0.02
bone	0.85 ± 0.21	0.33 ± 0.06	0.16 ± 0.06	0.10 ± 0.03	0.11 ± 0.02	0.06 ± 0.02
brain	0.16 ± 0.09	0.06 ± 0.02	0.04 ± 0.01	0.02 ± 0.00	0.02 ± 0.01	0.01 ± 0.00
urine	5.5	14.6	13.9	22.9	31.5	28.0

[^{111}In]**20**

tissue	5 min	15 min	30 min	60 min	120 min	240 min
blood	6.66 ± 1.15	3.98 ± 0.05	2.18 ± 0.32	0.95 ± 0.11	0.47 ± 0.02	0.34 ± 0.07
heart	6.29 ± 1.79	8.68 ± 1.67	7.12 ± 1.47	6.14 ± 0.17	4.08 ± 0.22	3.09 ± 0.54
lung	4.63 ± 0.90	3.64 ± 0.21	2.45 ± 0.07	1.72 ± 0.15	1.32 ± 0.07	0.99 ± 0.20
liver	3.91 ± 0.46	4.94 ± 0.06	4.37 ± 0.33	4.44 ± 0.34	4.51 ± 0.47	4.32 ± 0.25
spleen	2.88 ± 0.44	3.70 ± 0.69	3.91 ± 0.86	4.22 ± 0.89	2.45 ± 0.05	2.09 ± 0.78
pancreas	2.03 ± 0.30	2.83 ± 1.67	3.57 ± 0.69	3.32 ± 1.30	2.35 ± 1.35	2.02 ± 1.12
stomach	1.43 ± 0.28	2.40 ± 0.20	3.27 ± 1.07	2.92 ± 0.72	4.48 ± 0.84	2.78 ± 0.34
s. intestine	6.22 ± 0.66	11.74 ± 1.03	14.95 ± 0.78	12.55 ± 0.81	10.81 ± 2.18	9.36 ± 3.08
cecum	1.86 ± 0.06	2.86 ± 0.39	3.50 ± 0.72	3.45 ± 0.49	5.12 ± 0.62	6.66 ± 0.72
l. intestine	4.36 ± 0.71	7.84 ± 0.75	8.93 ± 0.54	9.22 ± 1.37	9.43 ± 1.31	7.54 ± 1.12
kidney	5.85 ± 1.01	4.45 ± 0.31	5.04 ± 2.87	3.32 ± 0.59	2.66 ± 0.26	2.40 ± 0.21
muscle	1.04 ± 0.17	0.66 ± 0.05	0.52 ± 0.09	0.35 ± 0.03	0.22 ± 0.01	0.18 ± 0.02
bone	1.15 ± 0.52	0.64 ± 0.18	0.39 ± 0.05	0.33 ± 0.08	0.16 ± 0.06	0.18 ± 0.03
brain	0.21 ± 0.06	0.14 ± 0.01	0.08 ± 0.01	0.05 ± 0.00	0.03 ± 0.01	0.03 ± 0.00
urine	3.6	14.8	11.4	25.3	33.1	31.2

[^{111}In]**18**

tissue	5 min	15 min	30 min	60 min	120 min	240 min
blood	8.09 ± 0.45	3.84 ± 0.53	2.17 ± 0.19	0.98 ± 0.24	0.54 ± 0.08	0.25 ± 0.12
heart	7.22 ± 0.74	7.38 ± 0.94	7.41 ± 2.08	7.92 ± 1.75	5.94 ± 0.18	4.56 ± 0.41
lung	6.47 ± 0.80	3.47 ± 0.43	2.40 ± 0.11	1.87 ± 0.45	1.45 ± 0.34	1.02 ± 0.14
liver	6.24 ± 0.47	7.17 ± 0.31	7.07 ± 0.40	6.29 ± 1.19	3.89 ± 0.48	3.15 ± 0.71
spleen	3.42 ± 1.69	3.15 ± 0.73	2.92 ± 0.69	2.82 ± 0.56	3.39 ± 0.43	3.32 ± 1.60
pancreas	2.24 ± 0.34	2.19 ± 0.37	3.12 ± 0.17	4.81 ± 1.65	3.02 ± 1.20	2.75 ± 1.09
stomach	1.73 ± 0.24	2.78 ± 0.88	3.22 ± 0.39	4.47 ± 1.12	3.99 ± 0.71	3.91 ± 0.97
s. intestine	9.09 ± 1.32	11.07 ± 0.70	15.07 ± 1.20	16.81 ± 0.67	16.73 ± 1.38	15.48 ± 1.97
cecum	2.06 ± 0.25	2.86 ± 0.32	4.13 ± 0.27	4.13 ± 0.87	5.29 ± 2.20	11.80 ± 3.59
l. intestine	6.28 ± 1.30	7.40 ± 0.60	9.18 ± 0.78	12.28 ± 1.95	9.80 ± 1.39	10.43 ± 2.28
kidney	8.86 ± 1.23	5.45 ± 1.55	3.66 ± 0.44	2.87 ± 0.59	2.64 ± 0.66	2.28 ± 0.19
muscle	1.55 ± 0.33	0.69 ± 0.13	0.53 ± 0.13	0.37 ± 0.05	0.25 ± 0.04	0.18 ± 0.02
bone	1.24 ± 0.23	0.50 ± 0.20	0.41 ± 0.09	0.23 ± 0.13	0.18 ± 0.03	0.13 ± 0.03
brain	0.28 ± 0.11	0.12 ± 0.03	0.08 ± 0.01	0.04 ± 0.00	0.04 ± 0.01	0.03 ± 0.00
urine	6.4	15.8	24.6	29.2	30.7	35.0

[a] Values are %ID/g (means ± SD, $n = 3$), except for urine which is %ID.

during assays, and it may be one contributing factor to the observed affinities and selectivities.

Direct Binding Assays. Findings from the competition experiments were confirmed by direct determination of binding parameters for [^{111}In]**17** and [^{111}In]**19** in mouse brain membranes. "Cold" saturation studies using a low, fixed amount of [^{111}In]**17** in the presence of increasing concentrations of **17** gave a measured K_d of 7.21 ± 0.94 nM and a site density (B_{max}) of 82.7 ± 8.1 fmol/mg protein (data not shown). "Hot" saturation studies using increasing concentrations of [^{111}In]**19**, intentionally lowered to 1500 mCi/μmol by addition of **19**, gave a K_d of 0.16 ± 0.01 nM and a B_{max} of 122 ± 1.3 fmol/mg protein (Figure 3A). Rosenthal transformations of both data sets were linear, consistent with labeling of a single binding site. Incubation times at 37 °C for these assays were based upon association studies showing that 45 min and 2 h were necessary to achieve steady state for [^{111}In]**17** and [^{111}In]**19**, respectively (data not shown). The K_d values are in good agreement with the K_i values from the δ opioid receptor competition binding assays (Table 1), and the B_{max} values are near the 83.9 fmol/mg protein previously obtained in whole mouse brain using [^{3}H]NTI.[26a]

The specific binding of both [^{111}In]**17** and [^{111}In]**19** was inhibited potently by δ, but not by μ or κ, opioid receptor ligands. K_i values for δ selective ligands against [^{111}In]**17** were 0.28 ± 0.09 nM for NTI and 3.68 ± 1.10 nM for the peptide DPDPE (data not shown). Against [^{111}In]**19**, K_i values were 0.16 ± 0.01 nM for NTI and 4.19 ± 0.24 nM for DPDPE (Figure 3B). Hill coefficients were near unity in each case, ranging from 0.95 to 1.10. Neither the μ selective peptide DAMGO, nor the κ selective arylacetamide U69,593, displaced the specific binding of [^{111}In]**17** or [^{111}In]**19** at 1.0−2.0 μM (data not shown). Further, specific binding of the complexes was not

Table 3. Effects of Pretreatments on In Vivo Uptake of [^{111}In]-Labeled Complexes **19**, **20**, and **18** in Male CD1 Mice[a]

[^{111}In]**19**

tissue	saline controls	naltrexone	complex **19**	NTI
stomach	5.24 ± 1.85	4.62 ± 2.24	2.48 ± 1.11	2.45 ± 3.08
s. intestine	9.18 ± 1.22	2.67 ± 0.65	1.52 ± 0.76	1.53 ± 0.68
cecum	2.16 ± 0.51	0.45 ± 0.14	0.13 ± 0.02	0.25 ± 0.19
l. intestine	5.65 ± 0.88	1.17 ± 0.15	0.21 ± 0.02	0.29 ± 0.04
heart	3.10 ± 0.60	0.52 ± 0.12	0.26 ± 0.03	0.30 ± 0.04
spleen	2.43 ± 0.32	0.58 ± 0.10	0.43 ± 0.11	0.61 ± 0.08
pancreas	1.53 ± 0.12	0.33 ± 0.10	0.22 ± 0.06	0.20 ± 0.08
lung	0.80 ± 0.10	0.61 ± 0.08	0.56 ± 0.03	0.64 ± 0.10
muscle	0.11 ± 0.02	0.09 ± 0.01	0.08 ± 0.02	0.11 ± 0.03
brain	0.02 ± 0.00	0.03 ± 0.00	0.03 ± 0.01	0.03 ± 0.01
liver	14.79 ± 1.18	18.58 ± 1.34	17.70 ± 1.78	16.25 ± 2.21
kidney	1.71 ± 0.36	1.93 ± 0.31	3.68 ± 2.50	3.38 ± 2.51
urine	22.2	31.6	24.7	35.3
blood	0.28 ± 0.05	0.78 ± 0.14	0.61 ± 0.05	1.45 ± 1.01

[^{111}In]**20**

tissue	saline controls	naltrexone	complex **20**	NTI
stomach	3.89 ± 0.67	2.63 ± 0.84	0.68 ± 0.17	0.63 ± 0.06
s. intestine	13.91 ± 2.18	4.65 ± 0.16	1.50 ± 0.27	1.10 ± 0.07
cecum	4.28 ± 0.73	1.48 ± 0.10	0.56 ± 0.14	0.40 ± 0.04
l. intestine	10.23 ± 1.10	4.35 ± 0.66	1.22 ± 0.29	0.99 ± 0.04
heart	7.28 ± 0.99	2.30 ± 0.53	1.77 ± 0.34	1.00 ± 0.07
spleen	5.01 ± 1.22	1.57 ± 0.24	1.34 ± 0.32	0.81 ± 0.10
pancreas	3.76 ± 1.46	1.35 ± 0.62	1.18 ± 0.19	0.74 ± 0.14
lung	1.92 ± 0.05	2.11 ± 0.31	3.47 ± 1.04	2.01 ± 0.13
muscle	0.40 ± 0.07	0.38 ± 0.04	0.72 ± 0.18	0.37 ± 0.02
brain	0.07 ± 0.03	0.07 ± 0.01	0.13 ± 0.04	0.08 ± 0.00
liver	4.36 ± 0.37	7.07 ± 0.62	4.73 ± 0.71	6.99 ± 0.23
kidney	5.05 ± 1.63	4.08 ± 0.73	9.12 ± 3.96	4.29 ± 0.589
urine	22.0	34.0	23.2	41.4
blood	1.22 ± 0.12	2.10 ± 0.25	3.88 ± 0.65	2.23 ± 0.20

[^{111}In]**18**

tissue	saline controls	naltrexone	complex **18**	NTI
stomach	3.43 ± 0.64	1.57 ± 0.30	1.69 ± 0.78	1.01 ± 0.29
s. intestine	15.62 ± 1.48	4.20 ± 0.43	2.10 ± 0.54	2.26 ± 0.51
cecum	4.15 ± 0.76	1.32 ± 0.18	0.44 ± 0.10	0.27 ± 0.04
l. intestine	11.97 ± 1.46	4.06 ± 0.23	0.98 ± 0.15	0.79 ± 0.08
heart	6.08 ± 0.65	1.83 ± 0.30	1.28 ± 0.24	0.85 ± 0.06
spleen	3.12 ± 1.06	1.19 ± 0.19	0.98 ± 0.13	0.61 ± 0.10
pancreas	3.35 ± 0.56	0.90 ± 0.36	1.00 ± 0.19	0.76 ± 0.29
lung	1.79 ± 0.09	1.68 ± 0.18	2.70 ± 0.49	1.65 ± 0.08
muscle	0.36 ± 0.03	0.28 ± 0.02	0.61 ± 0.18	0.29 ± 0.05
brain	0.05 ± 0.01	0.07 ± 0.02	0.09 ± 0.01	0.06 ± 0.01
liver	6.63 ± 0.94	8.81 ± 1.33	9.87 ± 1.46	8.77 ± 0.56
kidney	2.75 ± 0.18	3.62 ± 0.40	9.00 ± 2.90	4.02 ± 0.67
urine	27.3	35.7	21.8	33.3
blood	0.79 ± 0.10	1.44 ± 0.09	3.72 ± 1.28	1.69 ± 0.09

[a] Values are %ID/g (means ± SD, $n = 4$) 60 min after radioligand administration. Urine is %ID. Naltrexone (10 μmol/kg), indium(III) complexes (5 μmol/kg), and NTI (5 μmol/kg) were given 5 min prior to radioligand.

inhibited by haloperidol at 1.0−2.0 μM, concentrations that would block significant contributions from serotonin 5-HT$_2$, dopamine D$_{1-4}$, σ_{1-2}, or α_1-adrenergic receptors.[31,33] Thus, these [^{111}In]complexes selectively label δ opioid receptors in vitro when used near their K_d values.

Autoradiography. The δ opioid receptor binding of [^{111}In]-**19** was investigated by autoradiography in order to extend the findings from homogenate assays. Although the [^{111}In]complexes were not designed for brain studies in vivo, we used sections from mouse brain since the populations of the multiple opioid receptors are well-defined. Appropriate topography for selective labeling of δ sites was observed (Figure 4), with the levels of radioactivity being high in striatal and cortical regions, intermediate in the hippocampal formation, low in thalamus and colliculi, and barely detectable in cerebellum. This rank order is in full accord with δ opioid receptor densities known from autoradiographic studies of mouse brain using [^{125}I]-[D-Ala^2]deltorphin-I[34] and of rat brain using [^{3}H]-NTI.[35] The δ opioid receptor distribution of [^{111}In]**19** was abolished by the δ selective naltriben (5 nM), but not by 50-fold higher concentrations of μ selective DAMGO or κ selective U69,593.

In Vivo Pharmacokinetics. Pharmacokinetic profiles for the [^{111}In]complexes were determined after iv administration to male CD1 mice. Data for high-affinity complexes [^{111}In]**18**−[^{111}In]-**20** is given in Table 2, and a graphical representation for [^{111}In]**18** is shown in Figure 5. Biodistributions reflect the effect of relative lipophilicities on first-pass extraction, coupled with clearance from tissues having few δ opioid receptors and prolonged retention in peripheral organs that are rich in δ opioid receptors (vide infra). None of the [^{111}In]complexes penetrated the brain in accord with their high molecular weights and hydrogen bonding ability. Bone uptakes were low, a finding consistent with good metabolic stability. Negligible radioactivity, <0.2% of the injected dose (ID), was noted in feces during the studies. Cumulative urinary excretion of radioactivity was nearly

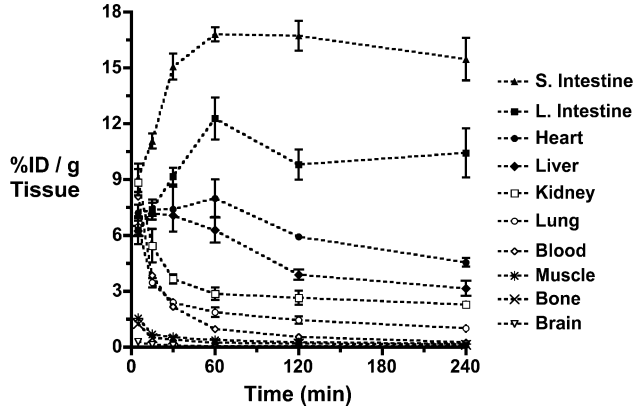

Figure 5. Temporal biodistribution after intravenous administration of [^{111}In]**18** (3.5 μCi) to male CD1 mice. Values are %ID/g (means ± SEM, $n = 3$).

complete for all radioligands within the first 60 min and ranged from 22.9% to 29.2% ID.

Initial blood levels of radioactivity, as well as the 5 min uptakes by lung, heart, spleen, pancreas, intestines, and skeletal muscle, increased with radioligand lipophilicity (cf. Tables 1 and 2). The most lipophilic complex, [^{111}In]**18** (log $D_{7.4}$ −1.79), displayed 2- to 3-fold higher levels of uptake than the least lipophilic complex [^{111}In]**19** (log $D_{7.4}$ −2.74). Correlation of these early volumes of distribution with hydrophobicity is presumably due to differential membrane permeability and binding to serum proteins. After extraction, radioactivity for heart, spleen, pancreas, and the gastrointestinal tract, organs with appreciable δ opioid receptors,[12,13,36−39] remained stable or increased over time (Table 2, Figure 5). By contrast, all three radioligands showed rapid clearance from blood, lung, skeletal muscle, and kidney in accord with low levels of δ opioid receptors.[11a,b,37,40] These data were fitted by monoexponential curves ($r = 0.89-0.99$; data not shown; cf. Figure 5).

Liver uptakes for [^{111}In]**18** and [^{111}In]**20**, the most lipophilic complexes, were similar and low (4 − 7% ID/g; Table 2). Higher uptakes were shown by [^{111}In]**19** (Table 2) and [^{111}In]-**17**, the least lipophilic complexes, with particularly high values for [^{111}In]**17** (24.0% ID/g, 5 min; 12.1% ID/g, 240 min; data not shown). Such differences might rise from substituent effects on liver metabolism or carrier-mediated transport.[41] However, a simple explanation is higher binding of [^{111}In]**18**/[^{111}In]**20** to serum proteins leads to reduced availability for hepatocellular uptake compared to [^{111}In]**17**/[^{111}In]**19** as previously shown for doxorubicin analogues.[42] Thus, an optimal range of lipophilicity exists that reduces liver uptake and might improve SPECT image quality. Other biodistribution data for [^{111}In]**17** were unremarkable, presumably due to lower affinity for δ opioid receptors. Radioactivity cleared quickly from blood and most peripheral organs (data not shown), with retention for the intestines (ca. 15% ID/g, 60 min).

In Vivo Pharmacology. The pharmacology of the [^{111}In]-complexes was assessed by pretreatment of mice with various opioids and determination of tissue radioactivity 60 min later. As shown in Table 3 and Figure 6, uptakes of the high-affinity complexes [^{111}In]**18**−[^{111}In]**20** in heart, spleen, pancreas, and all regions of the gastrointestinal tract were blocked by the "universal" opioid receptor antagonist naltrexone (10 μmol/kg), saturated by the corresponding cold complex (5 μmol/kg), and fully inhibited by the δ selective NTI (5 μmol/kg). The only exception was the stomach of [^{111}In]**19** where coefficients of variation were high, and inhibition did not reach statistical significance. Using NTI blockade to define nonspecific binding, levels of specific binding to δ opioid receptors were 86−90% in heart, 77−87% in pancreas, 75−84% in spleen, and 83−94% across the three intestinal regions. For low-affinity [^{111}In]**17**, gut levels were reduced 22−52% by naltrexone, cold complex, and NTI, but reached significance only for naltrexone and cold complex (data not shown). By contrast, the inhibitors had either little effect on, or in some cases increased, radioactivity levels in blood, lung, kidney, and skeletal muscle (Table 3, Figure 6). We attribute these elevations to greater radiotracer availability for nonspecific partitioning as a consequence of blockade of specific δ opioid receptor binding in other organs. The cold complexes exerted pronounced effects compared to NTI or naltrexone. We conclude that the [^{111}In]complexes exhibit a component of binding in vivo that is saturable, but nonspecific to classical opioid receptors, in as yet unidentified peripheral regions.

There are few radioligand binding studies of peripheral δ opioid receptors in vitro or in vivo that can be used for direct comparison to the data obtained with these [^{111}In]complexes in mouse. However, significant populations of δ sites are known for organ systems where the [^{111}In]complexes showed appreciable specific binding. Radioligand binding studies have demonstrated δ and κ, but not μ, opioid receptors in membranes from adult rat heart.[36] Likewise, δ and κ mRNA expression has been found for human heart,[12b] and cardioprotective activation of δ sites is of clinical interest.[12] Binding studies have shown δ opioid receptors in islets of Langerhans from rat pancreas[37] and in rat splenocytes.[38] The significance of opioid receptors to gastrointestinal function is well recognized, and multiple opioid receptors are distributed throughout the stomach and intestines of mice, rats, guinea pigs, dogs, and human beings.[13,39] The most detailed studies are in porcine gut, where δ sites having picomolar affinity for [^{3}H]NTI are located in high densities (~60 fmol/mg protein) in all intestinal segments.[39d]

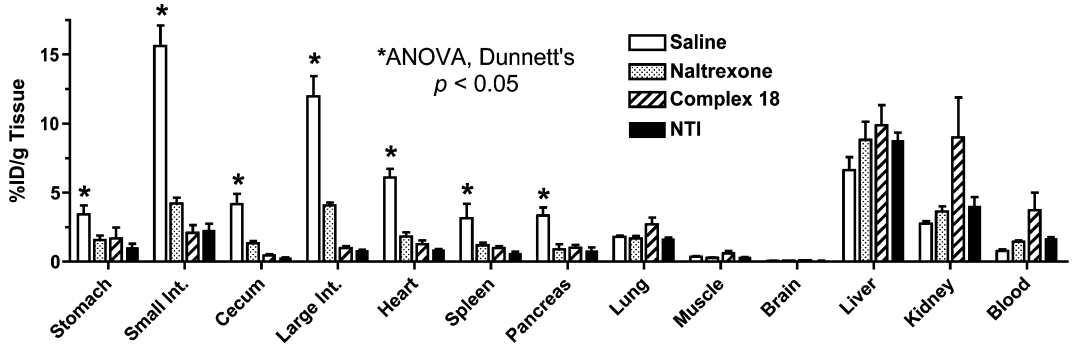

Figure 6. Inhibitor effects on in vivo uptake of [^{111}In]**18** at 60 min in male CD1 mice. Values are %ID/g (means ± SD, $n = 4$). Naltrexone (10 μmol/kg), **18** (5 μmol/ kg), and NTI (5 μmol/kg) were given 5 min prior to radioligand. *Tissues showing significant inhibition of radioligand binding.

In keeping with the pharmacokinetic and pharmacologic data for the [^{111}In]complexes, δ opioid receptors are not thought to be highly expressed by lung, skeletal muscle, liver, or kidney. Detection of δ sites was not possible in normal mouse lung homogenates by radioligand binding,[11a] and gene expression was not observed in normal human lung.[11b] Radioligand binding to δ sites in rat lung has been reported,[43] raising the possibility of species differences. Skeletal muscle is typically considered an opioid "blank,"[37] though low levels of functional δ sites can be localized on mouse muscle fibers by autoradiography.[40] Opioid peptides are present in rat liver extracts, but classical opioid receptors are not found in liver preparations.[37] Opioid drugs influence renal function,[44] and δ receptor agonists increase urinary flow and sodium excretion in rats as long as renal nerves are intact.[45] Functional δ opioid receptors must be present, but so far only transcripts have been reported in rat kidney.[46] Similarly, the low levels of functional opioid receptors expressed by cells of the immune system are difficult to detect by conventional radioligand binding assays.[47] The high specific activity, affinity, and selectivity of the [^{111}In]-labeled conjugates of NTI may present an opportunity for sensitive in vitro assays of δ opioid receptors in such systems, although the 2.8 day half-life imposes constraints on routine usage.

Overall, the in vivo data for complexes [^{111}In]**18**−[^{111}In]**20** is consistent with a high level of specific labeling of δ opioid receptors throughout the periphery of mice. Other in vivo studies of radioligand binding to peripheral opioid receptors have been more limited. The δ opioid peptide [^{3}H]DPDPE showed persistent uptake (~30% ID) in the small intestines of mice for 1−2 h.[48] However, blocking studies were not performed to differentiate hepatobiliary clearance from specific receptor binding. An in vivo study of the δ pseudopeptide, [^{125}I]ITIPP-(ψ), in nude mice bearing small cell lung cancer xenografts showed uptake in tumor, intestines, and liver that was inhibited (40−63%) by non-radioactive TIPP(ψ).[49] The data suggests specific binding to δ sites. Yet, as noted by the authors, only a single inhibitor, closely related in structure to the radiotracer, was employed. A radioiodinated diprenorphine showed in vivo uptake by breast cancer xenografts, intestines, and heart of immunodeficient mice that could be blocked by naltrexone (23−59%).[50] This radioligand, however, is not selective for a single type of opioid receptor, a limited inhibition profile was reported, and significant metabolic degradation was observed.

Conclusions. We have identified a series of hydrophilic [^{111}In]-labeled DOTA and DO3A conjugates of NTI that exhibit picomolar affinities and excellent selectivity for δ opioid receptors in vitro and show high levels of specific binding to peripheral δ opioid receptors in vivo. These [^{111}In]complexes seem well suited for studies of cardiac, intestinal, and other peripheral δ opioid receptors by SPECT, have the potential for noninvasive characterization of cancers that express these sites, and might aid in certain new drug development efforts. Extensions to include ligands labeled with a variety of other radiometals also should be possible.

Experimental Section

General Information. Reagents and solvents were the best grades available and were used as received. NTI was prepared[5] from naltrexone·HCl (Mallinckrodt, Inc.) and converted[6a] to *p*-toluenesulfonate ester **2** as previously reported. DO3A was prepared from 1,4,7,10-tetraazacyclododecane-1,4,7-tris(*t*-butyl acetate) (Macrocyclics, Inc.) by treatment with neat TFA,[21] and it was characterized by elemental analysis as DO3A·2TFA. DOTA-NHS was from Macrocyclics, Inc. Naltriben mesylate, NTI·HCl, DAMGO, DPDPE, and U69,593 were from Sigma-RBI. [^{111}In]Cl_3 was from Mallinckrodt, Inc., [^{3}H]NTI was from Perkin-Elmer, and [^{3}H]-DAMGO and [^{3}H]U69,593 were from Amersham Biosciences. High-resolution mass spectroscopy (HRMS) by electron impact (EI) or electrospray (ESI) mode was done at the University of Minnesota. ^{1}H NMR spectra were obtained at the University of Missouri, Department of Chemistry, on a Bruker DRX 300 MHz spectrometer. Chemical shifts are parts per million (δ) relative to residual solvent ($CHCl_3$, 7.24 ppm; HOD, 4.80 ppm; CD_2HCN, 1.94 ppm), with coupling constants (*J*) in hertz (Hz). Elemental analyses (Atlantic Microlab, Inc.) agreed with calculated values (±0.4%). Normal-phase silica gel (<230 mesh; Merck 7729) and reversed-phase C18 (35-75 μm; Analtech) column chromatography were done under N_2. TLC was done on Macherey-Nagel silica gel 60 UV254 (250 μm) or Whatman reversed-phase MKC18F 60 Å plates. Animal studies were done humanely in compliance with National Institutes of Health guidelines and with Institutional Animal Care and Use Committee approvals.

17-(Cyclopropylmethyl)-6,7-didehydro-4,5α-epoxy-3-(*p*-tosyloxy)-14-hydroxy-1′-(3″,3″-dimethoxypropyl)indolo[6,7:2′,3′]-morphinan (3). An ice-cold solution of 2[6a] (0.70 g, 1.2 mmol) and 3-bromopropionaldehyde dimethylacetal (0.94 mL, 6.9 mmol) in anhydrous DMF (7 mL) under argon was treated with powdered NaH (0.13 g, 5.0 mmol) under stirring. The mixture was warmed to room temperature, stirred 2 h, and partitioned between saturated sodium carbonate buffer (55 mL, pH 9.5) and EtOAc (30 mL). The organic layer was washed with buffer (4 × 20 mL), dried (Na_2SO_4), filtered, and concentrated. Silica gel chromatography (EtOAc/cyclohexane, 1:1; 1% Et_3N) gave **3** (0.64 g, 77%) as a white foam. HRMS-EI *m/z* calcd for $C_{38}H_{42}N_2O_7S$ $[M + H]^+$ 671.2785; found 671.2783. Anal. ($C_{38}H_{42}N_2O_7S·0.5H_2O$) C, H, N.

17-(Cyclopropylmethyl)-6,7-didehydro-4,5α-epoxy-3,14-dihydroxy-1′-(3″,3″-dimethoxypropyl)indolo[6,7:2′,3′]morphinan (4). A stirred solution of **3** (0.76 g, 1.1 mmol) in *i*-PrOH (50 mL) was treated with 1 N NaOH (25 mL) and brought to reflux under argon. After 15 h the mixture was cooled, brought to pH 9.5 with 1 N HCl (20 mL), diluted with brine (100 mL), and extracted with CH_2Cl_2 (5 × 20 mL). Combined extracts were dried (Na_2SO_4), filtered, and concentrated. Silica gel chromatography (EtOAc/cyclohexane, 1:1; 1% Et_3N) gave **4** (0.50 g, 83%) as an off-white solid. HRMS-EI *m/z* calcd for $C_{31}H_{36}N_2O_5$ $[M + H]^+$ 517.2697; found 517.2728. Anal. ($C_{31}H_{36}N_2O_5·1.5H_2O$) C, H, N.

17-(Cyclopropylmethyl)-6,7-didehydro-4,5α-epoxy-3,14-dihydroxy-1′-(2″-formylethyl)indolo[6,7:2′,3′]morphinan (5). A solution of **4** (0.34 g, 0.64 mmol) and *p*-TsOH·H_2O (0.26 g, 1.3 mmol) in acetone (9 mL) was refluxed 3 h under argon. The mixture was cooled, concentrated, and partitioned between sodium carbonate buffer (10 mL) and EtOAc (20 mL). The organic layer was washed with carbonate buffer, dried (Na_2SO_4), filtered, and concentrated to give **5** (0.32 g, ~74%) of 88% purity. This material was typically used without further purification due to losses (40%) upon chromatography. For characterization, **5** was purified by C18 chromatography (CH_3CN:H_2O, 30:70, 0.1% TFA) and partitioned between EtOAc and carbonate buffer. The organic extracts were dried (Na_2SO_4), filtered, and concentrated to give the free base. HRMS-ESI *m/z* calcd for $C_{29}H_{30}N_2O_4$ $[M + H]^+$ 471.2284; found 471.2293. Anal. ($C_{29}H_{30}N_2O_4·0.5H_2O$) C, H, N.

17-(Cyclopropylmethyl)-6,7-didehydro-4,5α-epoxy-3,14-dihydroxy-1′-(10‴-[3″-propyl]-[1‴,4‴,7‴,10‴-tetraazacyclododecane-1‴,4‴,7‴-triacetic acid])indolo[6,7:2′,3′]morphinan; *N*1′-(DO3A-propyl)NTI (6). A suspension of crude **5** (66 mg, 98 μmol), DO3A·2TFA (0.15 g, 0.26 mmol) and Et_3N (265 μL, 1.89 mmol) in CH_3CN (1.3 mL) under argon was treated with $NaBH(OAc)_3$ (46 mg, 0.21 mmol) and stirred 5 h at room temperature. The reaction was quenched with H_2O (0.25 mL) and concentrated. The residue was dissolved (CH_3CN:H_2O, 50:50, 1% TFA; 3 mL) and taken to dryness three times. A solution (0.1% TFA) was then loaded on a C18 column (1 × 8 cm) and eluted with CH_3CN:H_2O (30:70, 0.1% TFA). Similar fractions were combined, concentrated, diluted with H_2O, and lyophilized to give **6** (102 mg, 87%) as a white powder. HRMS-ESI *m/z* calcd for $C_{43}H_{56}N_6O_9$ $[M + H]^+$ 801.4182; found

801.4191. *m/z* calcd for $[M + Na]^+$ 823.4006; found 823.4006. Anal. ($C_{43}H_{56}N_6O_9 \cdot 3TFA \cdot 3H_2O$) C, H, N, F.

17-(Cyclopropylmethyl)-6,7-didehydro-4,5α-epoxy-3-(*p*-tosyloxy)-14-hydroxy-1′-(5″-cyanopentyl)indolo[6,7:2′,3′]morphinan (7). An ice-cold solution of **2** (1.39 g, 2.44 mmol) and 6-bromohexanenitrile (1.02 mL, 7.31 mmol) in anhydrous DMF (14 mL) under argon was treated with powdered NaH (0.12 g, 4.9 mmol) under vigorous stirring. The mixture was warmed to room temperature, stirred 1 h, and then partitioned between sodium carbonate buffer (40 mL) and EtOAc (100 mL). The organic layer was washed with carbonate buffer (4 × 30 mL), dried (Na_2SO_4), filtered, and concentrated. Silica gel chromatography (EtOAc/cyclohexane, 2:3; 1% Et_3N) gave **7** (1.56 g, 96%) as a white foam. HRMS-ESI *m/z* calcd for $C_{39}H_{41}N_3O_5S$ $[M + H]^+$ 664.2840; found 664.2868. *m/z* calcd for $[M + Na]^+$ 686.2659; found 686.2644. Anal. ($C_{39}H_{41}N_3O_5S$) C, H, N.

17-(Cyclopropylmethyl)-6,7-didehydro-4,5α-epoxy-3-(*p*-tosyloxy)-14-hydroxy-1′-(5″-formylpentyl)indolo[6,7:2′,3′]morphinan (8). A solution of DIBAL-H in toluene (3.7 mL, 1.0 M) was added over 1 min to a stirred solution of **7** (0.41 g, 0.62 mmol) in CH_2Cl_2 (8 mL) at room temperature under argon. After 15 min, the mixture was quenched by dropwise addition of 3 N HCl (10 mL), and diluted with CH_3CN:H_2O (50:50, 1% 3N HCl) until homogeneous. This solution was loaded on a C18 column (2.5 × 12 cm) and eluted with CH_3CN:H_2O (50:50, 1% 3 N HCl). Similar fractions, giving a brown color with vanillin−sulfuric acid spray reagent, were pooled, concentrated, and then purified a second time using the same conditions. The residue was partitioned between CH_2Cl_2 (5 × 25 mL) and saturated sodium carbonate buffer (50 mL). The combined extracts were dried (Na_2SO_4), filtered, and concentrated to give **8** (167 mg, 40%) as a white solid. HRMS-ESI *m/z* calcd for $C_{39}H_{42}N_2O_6S$ $[M + H]^+$ 667.2836; found 667.2865. Anal. ($C_{39}H_{42}N_2O_6S \cdot 0.4H_2O$) C, H, N.

17-(Cyclopropylmethyl)-6,7-didehydro-4,5α-epoxy-3-(*p*-tosyloxy)-14-hydroxy-1′-(10‴-[6″-hexyl]-[1‴,4‴,7‴,10‴-tetraazacyclododecane-1‴,4‴,7‴-triacetic acid])indolo[6,7:2′,3′]morphinan (9). A suspension of **8** (105 mg, 156 μmol), DO3A·2TFA (0.12 g, 0.20 mmol), and Et_3N (220 μL, 0.83 mmol) in DMF (2.0 mL) under argon was treated with $NaBH(OAc)_3$ (52 mg, 0.24 mmol) and stirred 1 h at room temperature. The reaction was quenched with H_2O (0.10 mL), and concentrated. The residue was treated with H_2O (10 mL), neat TFA (100 μL), and CH_3CN (2.5 mL) and then purified by gradient C18 column chromatography (H_2O to CH_3CN:H_2O, 50:50; 0.1% TFA). Similar fractions were combined, concentrated, diluted with H_2O, and lyophilized to give **9** (140 mg, 68%) as a white powder. HRMS-ESI *m/z* calcd for $C_{53}H_{68}N_6O_{11}S$ $[M + H]^+$ 997.4740; found 997.4736. *m/z* calcd for $[M + Na]^+$ 1019.4559; found 1019.4570. Anal. ($C_{53}H_{68}N_6O_{11}S \cdot 2.5TFA \cdot 2H_2O$) C, H, N, F.

17-(Cyclopropylmethyl)-6,7-didehydro-4,5α-epoxy-3,14-dihydroxy-1′-(10‴-[6″-hexyl]-[1‴,4‴,7‴,10‴-tetraazacyclododecane-1‴,4‴,7‴-triacetic acid])indolo[6,7:2′,3′]morphinan; *N*1′-(DO3A-hexyl)NTI (10). A solution of **9** (100 mg, 76 μmol) in 1 N NaOH (10 mL) was refluxed 16 h under argon. The reaction was chilled, treated dropwise with 30% TFA (3 mL), and then diluted with water (5 mL) and CH_3CN (4 mL). The mixture was loaded on a C18 column (1 × 8 cm), and eluted with aqueous TFA (0.1%, 10 mL) followed by CH_3CN:H_2O (40:60, 0.1% TFA). A second C18 purification (CH_3CN:H_2O, 25:75, 0.1% TFA) was done, and the usual isolation procedure followed by lyophilization gave **10** (60 mg, 64%) as white flakes. HRMS-ESI *m/z* calcd for $C_{46}H_{62}N_6O_9$ $[M + H]^+$ 843.4651; found 843.4695. *m/z* calcd for $[M + Na]^+$ 865.4470; found 865.4488. Anal. ($C_{46}H_{62}N_6O_9 \cdot 3TFA \cdot 2.75H_2O$) C, H, N, F.

17-(Cyclopropylmethyl)-6,7-didehydro-4,5α-epoxy-3-(*p*-tosyloxy)-14-hydroxy-1′-[3″-(*N*-phthalimido)propyl]indolo[6,7:2′,3′]-morphinan (11). An ice-cold solution of **2** (0.96 g, 1.69 mmol) and *N*-(3-bromopropyl)phthalimide (3.67 g, 13.4 mmol) in anhydrous DMF (10 mL) under argon was treated with powdered NaH (0.28 g, 11 mmol) under vigorous stirring. The mixture was allowed to warm to ambient temperature, stirred for 2 h, and then partitioned between saturated sodium carbonate buffer (35 mL) and EtOAc (70 mL). The organic layer was washed with carbonate buffer (4 × 30 mL), dried (Na_2SO_4), filtered, and concentrated. The yellow syrup was purified by silica gel chromatography (EtOAc/cyclohexane, 2:3; 1% Et_3N) to give **11** (1.07 g, 84%) as a white foam. HRMS-ESI *m/z* calcd for $C_{44}H_{41}N_3O_7S$ $[M + H]^+$ 756.2743; found 756.2775. Anal. ($C_{44}H_{41}N_3O_7S$) C, H, N.

17-(Cyclopropylmethyl)-6,7-didehydro-4,5α-epoxy-3,14-dihydroxy-1′-(3″-aminopropyl)indolo[6,7:2′,3′]morphinan (12). A suspension of **11** (0.54 g, 0.71 mmol) in *i*-PrOH (23 mL) was treated with 1 N NaOH (17 mL) and brought to reflux under argon. After 15 h, the mixture was cooled in an ice bath and brought to pH 9.5 with 1 N HCl (20 mL). Solid NaCl was added, with swirling, until phases separated. The aqueous phase was extracted with *i*-PrOH (3 × 10 mL), and the extracts were concentrated. Cold CH_3CN (70 mL, 0.3% TFA) was added and then concentrated. The residue was loaded on a plug of C18, washed with H_2O (0.1% TFA), and then eluted with CH_3CN (0.1% TFA). Final purification was achieved by C18 chromatography (CH_3CN:H_2O, 25:75, 0.1% TFA) to give **12** (0.55 g, 93%) as a white powder. HRMS-ESI *m/z* calcd for $C_{29}H_{33}N_3O_3$ $[M + H]^+$ 472.2600; found 472.2601. Anal. ($C_{29}H_{33}N_3O_3 \cdot 3TFA \cdot H_2O$) C, H, N, F.

17-(Cyclopropylmethyl)-6,7-didehydro-4,5α-epoxy-3,14-dihydroxy-1′-(5″-cyanopentyl)indolo[6,7:2′,3′]morphinan (13). A stirred solution of **7** (1.49 g, 2.25 mmol) in 1,4-dioxane (17 mL) was treated dropwise with methanolic *n*-Bu_4NOH (7.7 mL, 1 M) and brought to reflux under argon. After 8 h, the mixture was cooled, quenched (3 N HCl, 2.5 mL), and partitioned between saturated sodium carbonate buffer (50 mL) and EtOAc (150 mL). The organic layer was washed with carbonate buffer (3 × 30 mL), dried (Na_2SO_4), filtered, and concentrated. Silica gel chromatography (EtOAc/cyclohexane, 2:3; 1% Et_3N) gave **13** (0.79 g, 68%) as a pale yellow powder. HRMS-ESI *m/z* calcd for $C_{32}H_{35}N_3O_3$ $[M + H]^+$ 510.2751; found 510.2775. Anal. ($C_{32}H_{35}N_3O_3 \cdot 0.5H_2O$) C, H, N.

17-(Cyclopropylmethyl)-6,7-didehydro-4,5α-epoxy-3,14-dihydroxy-1′-(6″-aminohexyl)indolo[6,7:2′,3′]morphinan (14). A solution of DIBAL-H in toluene (10 mL, 1.0 M) was added over 8 min to a stirred solution of **13** (0.50 g, 0.96 mmol) in CH_2Cl_2 (3.5 mL) at 0 °C under argon. After 3 h, the mixture was quenched by dropwise addition of 0.1 N HCl (12 mL) and taken to dryness under reduced pressure. The residue was diluted with CH_3CN:H_2O (35:65, 1% 3 N HCl; 20 mL), loaded on a C18 column (2.5 × 12 cm), and eluted with CH_3CN:H_2O (35:65, 1% 3 N HCl). Similar fractions, giving a pink color with vanillin−sulfuric acid spray reagent, were pooled, concentrated, and then purified again under the same conditions. Combined fractions were concentrated, diluted with H_2O, and lyophilized to give **14** (387 mg, 64%). HRMS-ESI *m/z* calcd for $C_{32}H_{39}N_3O_3$ $[M + H]^+$ 514.3070; found 514.3064. Anal. ($C_{32}H_{39}N_3O_3 \cdot 4HCl \cdot 4.5H_2O$) C, H, N.

17-(Cyclopropylmethyl)-6,7-didehydro-4,5α-epoxy-3,14-dihydroxy-1′-(10‴-[3″-acetamidopropyl]-[1‴,4‴,7‴,10‴-tetraazacyclododecane-1‴,4‴,7‴-triacetic acid])indolo[6,7:2′,3′]morphinan; *N*1′-(DOTA-propylamido)NTI (15). A mixture of **12** (209 mg, 0.251 mmol), DOTA-NHS (347 mg, 0.418 mmol), DMAP (10 mg, 82 μmol), and Et_3N (500 μL, 3.56 mmol) in CH_3CN (2.2 mL) was stirred 5 h at room temperature under argon and then concentrated. Cold H_2O (10 mL) and TFA (80 μL) were added and then concentrated. Gradient C18 chromatography (CH_3CN:H_2O, 25:75 to 35:65, 0.1% TFA) was performed twice to give **15** (225 mg, 74%) as an off-white powder after concentration, dilution with H_2O, and lyophilization. HRMS-ESI *m/2z* calcd for $C_{45}H_{59}N_7O_{10}$ $[M + 2H]^{2+}$ 429.7239; found 429.7259. Anal. ($C_{45}H_{59}N_7O_{10} \cdot 2.5TFA \cdot 3.5H_2O$) C, H, N, F.

17-(Cyclopropylmethyl)-6,7-didehydro-4,5α-epoxy-3,14-dihydroxy-1′-(10‴-[6″-acetamidohexyl]-[1‴,4‴,7‴,10‴-tetraazacyclododecane-1‴,4‴,7‴-triacetic acid])indolo[6,7:2′,3′]morphinan; *N*1′-(DOTA-hexylamido)NTI (16). A mixture of **14** (78 mg, 0.15 mmol), DOTA-NHS (190 mg, 0.229 mmol), DMAP (4.0 mg, 33 μmol), and Et_3N (210 μL, 1.49 mmol) in DMSO (1.2 mL) was stirred 1.5 h at room temperature under argon. Workup as described above, using gradient C18 chromatography (CH_3CN:H_2O, 10:90

to 30:70, 0.1% TFA), provided **16** (65 mg, 34%) as a shiny white powder after lyophilization. HRMS-ESI *m/z* calcd for $C_{48}H_{65}N_7O_{10}$ $[M + Na]^+$ 922.4685; found 922.4694. Anal. ($C_{48}H_{65}N_7O_{10}$·2.75TFA·3H_2O) C, H, N, F.

17-(Cyclopropylmethyl)-6,7-didehydro-4,5α-epoxy-3,14-dihydroxy-1′-(indium(III)-[10‴-[3″-propyl]-[1‴,4‴,7‴,10‴-tetraazacyclododecane-1‴,4‴,7‴-triacetate]])indolo[6,7:2′,3′]morphinan; *N*1′-(In(III)-DO3A-propyl)NTI (17). A solution of **6** (35 mg, 29 μmol) and $InCl_3$ (9.6 mg, 43 μmol) in 0.4 M NH_4OAc (8.2 mL) was refluxed for 30 min, cooled to ambient temperature, and quenched with 0.1 N disodium EDTA (0.7 mL). This solution was loaded on a C18 column (1 × 8 cm) equilibrated with H_2O (0.1% TFA), washed with H_2O (0.1% TFA), and then eluted with CH_3CN:H_2O (30:70, 0.1% TFA). Similar fractions were combined, concentrated under reduced pressure, diluted with H_2O, and lyophilized to give (34 mg, 93%) as white flakes. ^{1}H NMR (D_2O, 300 MHz) δ 7.48 (d, *J* = 7.8 Hz, 2H, H4′, H7′), 7.31 (dd, *J* = 7.5 Hz, *J* = 7.8 Hz, 1H, H5′), 7.16 (dd, *J* = 7.5 Hz, *J* = 7.8 Hz, 1H, H6′), 6.84 (d, *J* = 8.2 Hz, 1H, H1/H2), 6.72 (d, *J* = 8.2 Hz, 1H, H1/H2), 5.93 (s, 1H, H5), 4.34 (m, 2H, H1″), 4.25 (m, 1H, H9), 3.67 (d, *J* = 17.4 Hz, 1H, H8α/H8β), 3.37−3.58 (m, 2H, H8α/H8β, H10β), 3.33 (m, 1H, H10α), 2.40−3.33 (m, 27H, H16ax/H16eq, H18, H3″, N−CH_2, N−CH_2C═O), 2.31 (m, 2H, H2″a, H16ax/ H16eq), 2.01 (m, 1H, H2″b), 1.81 (m, 2H, H15), 1.09 (m, 1H, H19), 0.82 (m, 2H, H20, H21), 0.48 (m, 2H, H20, H21). HRMS-ESI *m/z* calcd for $C_{43}H_{53}InN_6O_9$ $[M + H]^+$ 913.2986; found 913.2994. Anal. ($C_{43}H_{53}InN_6O_9$·2.5TFA·3H_2O) C, H, N, F.

17-(Cyclopropylmethyl)-6,7-didehydro-4,5α-epoxy-3,14-dihydroxy-1′-(indium(III)-[10‴-[6″-hexyl]-[1‴,4‴,7‴,10‴-tetraazacyclododecane-1‴,4‴,7‴-triacetate]])indolo[6,7:2′,3′]morphinan; *N*1′-(In(III)-DO3A-hexyl)NTI (18). A solution of **10** (23 mg, 19 μmol) and $InCl_3$ (9.0 mg, 41 μmol) in 0.4 M NH_4OAc (3.0 mL) was refluxed 30 min, cooled to ambient temperature, and quenched with 0.1 N disodium EDTA (0.4 mL). Workup as above, using C18 chromatography (CH_3CN:H_2O, 30:70, 0.1% TFA), gave **18** (17 mg, 72%) as white flakes after lyophilization. ^{1}H NMR (D_2O, 300 MHz) δ 7.53 (d, *J* = 7.6 Hz, 1H, H7′), 7.49 (d, *J* = 8.1 Hz, 1H, H4′), 7.31 (dd, *J* = 7.2 Hz, *J* = 8.1 Hz, 1H, H5′), 7.15 (dd, *J* = 7.2 Hz, *J* = 7.6 Hz, 1H, H6′), 6.82 (m, 2H, H1, H2), 5.96 (s, 1H, H5), 4.32 (m, 3H, H2″, H1″), 3.65 (d, *J* = 17.1 Hz, 1H, H10β), 3.62 (d, *J* = 17.4 Hz, 1H, H8α/H8β), 3.50 (s, 4H, N−CH_2C═O), 3.43 (m, 1H, H10α), 3.32 (d, *J* = 17.4 Hz, 1H, H8α/H8β), 2.81−3.29 (m, 15H, H16ax/H16eq, H18, N−CH_2, N−CH_2C═O), 2.45−2.80 (m, 9H, H16ax/H16eq, H6″, N−CH_2), 2.35 (m, 1H, H15ax/H15eq), 1.98 (m, 1H, H15ax/ H15eq), 1.87 (m, 2H, H2″), 1.38 (m, 2H, H3″), 1.12 (m, 3H, H19, H5″), 0.99 (m, 2H, H4″), 0.83 (m, 2H, H20, H21), 0.49 (m, 2H, H20, H21). HRMS-ESI *m/z* calcd for $C_{46}H_{59}InN_6O_9$ $[M + H]^+$ 955.3455; found 955.3464. *m/z* calcd for $[M + Na]^+$ 977.3275; found 977.3303. Anal. ($C_{46}H_{59}InN_6O_9$·2.2TFA·4H_2O) C, H, N, F.

17-(Cyclopropylmethyl)-6,7-didehydro-4,5α-epoxy-3,14-dihydroxy-1′-(indium(III)-[10‴-[3″-acetamidopropyl]-[1‴,4‴,7‴,-10‴-tetraazacyclododecane-1‴,4‴,7‴-triacetate]])indolo[6,7:2′,3′]morphinan; *N*1′-(In(III)-DOTA-propylamido)NTI (19). A solution of **15** (60 mg, 50 μmol) in 0.4 M NH_4OAc (6 mL) was treated with $InCl_3$ (13.2 mg, 60 μmol) in 0.05 N HCl (3.3 mL) at reflux for 30 min, cooled to ambient temperature, and quenched with 0.1 N disodium EDTA (0.9 mL). Workup as above, using C18 chromatography (CH_3CN:H_2O, 40:60, 0.1% TFA), gave **19** (43 mg, 69%) as white flakes after lyophilization. ^{1}H NMR (D_2O, 300 MHz) δ 7.48 (d, *J* = 7.8 Hz, 2H, H4′, H7′), 7.33 (dd, *J* = 7.3 Hz, *J* = 8.0 Hz, 1H, H5′), 7.13 (dd, *J* = 7.3 Hz, *J* = 7.6 Hz, 1H, H6′), 6.85 (m, 2H, H1, H2), 5.98 (s, 1H, H5), 4.40 (m, 2H, H1″), 4.30 (m, 1H, H9), 2.61-3.38 (m, 33H, H8, H10, H16ax/H16eq, H18, H3″, N−CH_2, N−CH_2C═O), 2.50 (m, 2H, H15ax/H15eq, H16ax/H16eq), 2.14 (m, 2H, H2″), 1.88 (m, 1H, H15ax/H15eq), 1.11 (m, 1H, H19), 0.83 (m, 2H, H20, H21), 0.48 (m, 2H, H20, H21). HRMS-ESI *m/z* calcd for $C_{45}H_{56}InN_7O_{10}$ $[M + H]^+$ 970.3206; found 970.3206. Anal. ($C_{45}H_{56}InN_7O_{10}$·2TFA·3H_2O) C, H, N, F.

17-(Cyclopropylmethyl)-6,7-didehydro-4,5α-epoxy-3,14-dihydroxy-1′-(indium(III)-[10‴-[6″-acetamidohexyl]-[1‴,4‴,7‴,10‴-tetraazacyclododecane-1‴, 4‴,7‴-triacetate]])indolo[6,7:2′,3′]-morphinan; *N*1′-(In(III)-DOTA-hexylamido)NTI (20). A solution of **16** (20 mg, 16 μmol) and $InCl_3$ (10.0 mg, 45 μmol) in H_2O (4.5 mL) was refluxed 45 min, cooled to ambient temperature, and quenched with 0.1 N disodium EDTA (0.75 mL). Workup as above, using C18 chromatography (CH_3CN:H_2O, 35:65, 0.1% TFA), gave **20** (20 mg, 95%) as white flakes after lyophilization. ^{1}H NMR (D_2O, 300 MHz) δ 7.45 (d, *J* = 7.3 Hz, 1H, H7′), 7.43 (d, *J* = 7.9 Hz, 1H, H4′), 7.25 (dd, *J* = 7.0 Hz, *J* = 7.9 Hz, 1H, H5′), 7.09 (dd, *J* = 7.0 Hz, *J* = 7.3 Hz, 1H, H6′), 6.82 (d, *J* = 8.2 Hz, 1H, H1/ H2), 6.77 (d, *J* = 8.2 Hz, 1H, H1/H2), 5.90 (s, 1H, H5), 4.24 (m, 3H, H9, H1″), 2.86−3.56 (m, 24H, H8α/H8β, H10, H16ax/H16eq, H18, H6″, N−CH_2C═O, N−CH_2), 2.35−2.79 (m, 11H, H8α/H8β, H15ax/H15eq, H16ax/H16eq, N−CH_2), 1.77 (m, 3H, H2″, H15ax/H15eq), 1.42 (m, 2H, H5″), 1.32 (m, 2H, H3″), 1.27 (m, 2H, H4″), 1.08 (m, 1H, H19), 0.79 (m, 2H, H20, H21), 0.44 (m, 2H, H20, H21). HRMS-ESI *m/z* calcd for $C_{48}H_{62}InN_7O_{10}$ $[M + H]^+$ 1012.3670; found 1012.3657. Anal. ($C_{48}H_{62}InN_7O_{10}$·2.25TFA·4H_2O) C, H, N, F.

General Radiolabeling Procedure. [^{111}In]**17**−[^{111}In]**20** were prepared by treating a water solution (50 μL) containing 50 μg of chelator (**6**, **10**, **15**, **16**) with 0.4 M NH_4OAc (30 μL) and aliquots of [^{111}In]$InCl_3$ (100−300 μL, 0.05 N HCl; 0.5 − 3.8 mCi) at 95 − 100 °C for 30 min in a septum-sealed glass vessel. Mixtures were cooled to room temperature, quenched with disodium EDTA (20 μL, 1.0 mM), and taken up in a syringe along with rinses (3 × 50 μL) of the vessel with the ternary mobile phase used for ion-pair HPLC purifications. Separations were run on a radial compression module (Nova-Pak C18, 8 × 100 mm, 6 μm) at a flow rate of 4 mL/min using a Waters system with UV (254 nm) detection interfaced with a flow-through NaI(Tl) scintillation detector (EE&G/Ortec). Conditions were used where complexes were resolved from precursors and from minor side products. Radioligand fractions were collected, diluted with an equal volume of water, and passed through an activated solid-phase extraction cartridge (Sep-Pak Light, *t*-C18) that was flushed with water (2.0 mL) and then with air. Elution with 70% EtOH (0.75−1.5 mL) furnished [^{111}In]**17**−[^{111}In]**20** in 55−83% yields. Radioligands were pure (>98%) by HPLC and coeluted with their respective non-radioactive complexes. Specific radioactivities were >3300 mCi/μmol based on minimum detectable mass (HPLC, 254 nm) in samples of known radioactivity (Capintec CRC-15W). Radioligands were stable for 24−48 h when stored in 70% EtOH at −20 °C in the dark, and nominal decomposition (∼5%) was noted during overnight storage at room temperature in saline (2−5% EtOH). Representative HPLC mobile phase compositions, retention times (t_R) and capacity factors (k') used during synthesis and analysis follow.

[^{111}In]**17**: t_R = 15.9 min, k' = 31; **6**: t_R = 12.4 min, k' = 24; mobile phase: MeOH (9.0%), MeCN (9.0%); H_2O (82%) with Et_3N (2.1%), HOAc (2.8%).

[^{111}In]**18**: t_R = 23.2 min, k' = 45; **10**: t_R = 18.0 min, k' = 35; mobile phase: MeOH (11.5%), MeCN (11.5%); H_2O (77%) with Et_3N (2.1%), HOAc (2.8%).

[^{111}In]**19**: t_R = 11.7 min, k' = 22; **15**: t_R = 16.8 min, k' = 32; mobile phase: MeOH (10.0%), MeCN (10.0%); H_2O (80%) with Et_3N (2.1%), HOAc (2.8%).

[^{111}In]**20**: t_R = 21.3 min, k' = 42; **16**: t_R = 26.0 min, k' = 51; mobile phase: MeOH (11.0%), MeCN (11.0%); H_2O (78%) with Et_3N (2.1%), HOAc (2.8%).

Log *D* Determinations. Log *D* values for freshly purified [^{111}In]complexes (3−5 μCi) were determined, in one session, by measuring distribution coefficients (*D*) between equal volumes (3.5 mL) of *n*-octanol and phosphate buffered saline (0.1 M, pH 7.4; PBS) where each phase had been saturated with the other. Mixtures were vortexed (30 s) and then centrifuged (2500 rpm, 5 min). Triplicate samples from the *n*-octanol (0.5 mL) and PBS (0.1 mL) phases were counted in an automated gamma counter, and *D* was determined as the ratio of mean CPM/mL for *n*-octanol compared to PBS. The process was repeated four times for each complex. Log *D* for [^{3}H]NTI, purified by HPLC, was determined similarly except the initial *n*-octanol solution was washed three times with

PBS to remove any hydrophilic contaminants. The *n*-octanol phase was partitioned, four times in sequence, with an equal volume of fresh PBS. After each partition, duplicate samples (0.1 mL) from each phase were counted by liquid scintillation to obtain the DPM/mL ratio.

Radioligand Binding Assays. Assays were conducted in membranes from fresh mouse (δ) or frozen guinea pig (μ, κ) brains using modifications of published procedures.[26,27] Nonspecific binding was defined for [^{3}H]NTI (δ) by NTI (1.0 μM), for [^{3}H]-U69,593 by U69,593 (10 μM), and for [^{3}H]DAMGO (μ) by DAMGO (5 μM). [^{3}H]DAMGO was used at 0.6 nM for 75 min at 25 °C, [^{3}H]U69,593 at 0.6 nM for 90 min at 25 °C, and [^{3}H]NTI at 0.1 nM for 90 min at 37 °C. Assays were run in duplicate glass test tubes using 10 inhibitor concentrations spaced equally on log scale and centered on the estimated IC_{50}. Protein concentrations of 0.3−0.5 mg/tube were used and were determined using the bicinchoninic acid assay against a bovine serum albumin (BSA) standard curve. Incubation buffer for μ and κ assays was 50 mM Tris-HCl (pH 7.4 at 25 °C). For δ assays, this buffer was supplemented with protease/peptidase inhibitors (50 μg/mL bacitracin, 30 μM bestatin, 10 μM captopril, 0.1 mM phenylmethylsulfonylfluoride) and 0.1% BSA. Assays were terminated by addition of ice-cold 50 mM Tris-HCl and filtered using a 48-well harvester (Brandel, Inc.) through glass fiber papers (GF/B) pretreated with polyethyleneimine (0.5%). Tubes and filter papers were washed with cold buffer (3 × 5 mL), and the papers were dried under vacuum. Scintillation counting (47% efficiency) was carried out after incubation of the discs with cocktail for 120 h. Data were analyzed using Radlig 6.0 (Biosoft, Inc.) and Prism 4.0 (GraphPad Software, Inc.). K_is were calculated from IC_{50}s by the Cheng−Prusoff equation using measured K_ds for [^{3}H]DAMGO (0.60 nM), [^{3}H]U69,593 (0.60 nM), and [^{3}H]NTI (0.061 nM) under these conditions. Association, saturation, and competition binding using [^{111}In]**17** and [^{111}In]**19** were performed at 37 °C using mouse brain membranes and δ receptor assay conditions as described above, except filter papers were counted immediately using an automated γ counter. The σ receptor assays were done using guinea pig brain membranes, [^{3}H](+)-pentazocine (σ_1), and [^{3}H]ditolylguanidine/200 nM (+)-pentazocine (σ_2) as reported elsewhere.[31]

Autoradiography. Male CD1 mice were killed by cervical dislocation, and their brains were removed and then frozen in isopentane at −55 °C. Horizontal sections (20 μm) were cut at −16 °C, and thaw-mounted on commercially subbed slides. After several days, sections were allowed to thaw and then incubated 15 min at 25 °C in 50 mM Tris-HCl (pH 7.4, 25 °C). Incubations were done using [^{111}In]**19** (0.1 nM, 1500 mCi/μmol) at 37 °C for 90 min in 50 mM Tris-HCl (pH 7.4, 25 °C; 0.1% BSA; protease inhibitor cocktail) to define total radioligand binding, along with baths containing naltriben (5 nM), DAMGO (250 nM), or U69,593 (250 nM). Slides were washed (3 × 10 min) in cold Tris-HCl (0.1% BSA), dipped (2 × 30 s) in cold water, air-dried, desiccated overnight in vacuo, and then apposed, along with polymer-based [^{125}I]-standards (20 μm; Amersham Corp.), against Kodak Biomax MR film for 30 h at room temperature. Films were developed, digitized, and analyzed (Inquiry System, Loats Assoc.). Optical densities for tissue sections were bracketed by values from the standards and did not exceed film response. Further image analysis and processing used program NIH Image (v. 1.63).

Biodistribution Studies. [^{111}In]-Labeled complexes (3−4 μCi) in sterile 0.9% saline (0.1 mL, 2% EtOH) were given by tail vein injection to sets of three male CD1 mice that were euthanized by cervical dislocation at intervals from 5 min to 4 h. Tissues were dissected, weighed, and counted using an automated γ counter, and data were compared to dilutions of the injected dose to obtain %ID/g wet weight of tissue. Blood was obtained by cardiac puncture. Small and large intestines were pressed free of contents, while cecum and stomach were measured as collected. Cumulative urinary excretion was determined by adding the radioactivity from an absorbent paper cage lining, a paper used under the animals during euthanasia, and the bladder. Pharmacologic studies followed the same protocols except groups of mice ($n = 4$) were pretreated by tail vein injections of saline (0.15 mL), cold complex (5 μmol/kg), naltrexone (10 μmol/kg), or NTI (5 μmol/kg) in saline (0.15 mL). Differences between control and treatment groups at 1 h were analyzed by ANOVA with a post hoc Dunnett's test.

Acknowledgment. We thank Ms. Lisa D. Watkinson and Mr. Terry L. Carmack for their capable work on biodistribution experiments and Ms. Emily A. Fergason for assistance with binding assays. We thank the National Cancer Institute (P50 CA 103130: Center for Single Photon-Emitting Cancer Imaging Agents) for support of this research and for a postdoctoral fellowship (R.A.D.) through the Career Development Core. We also acknowledge resources and facilities provided by the Harry S. Truman Memorial Veterans Hospital, the University of Missouri Life Sciences Mission Enhancement Program, and NSF CHE-95-31247 and NIH 1S10RR11962-01 grant awards for NMR instrumentation.

Supporting Information Available: Elemental analysis results for **3**−**20**, ^{1}H NMR data for **3**−**16**, and chart of the numbering conventions used in spectral descriptions. This material is available free of charge via the Internet at http://pubs.acs.org.

References

(1) Lever, J. R. PET and SPECT imaging of the opioid system: receptors, radioligands and avenues for drug discovery and development. *Curr. Pharm. Des.* **2007**, *13*, 33−49.

(2) (a) Lever, J. R.; Kinter, C. M.; Ravert, H.T.; Musachio, J. L.; Mathews, W. B.; Dannals, R. F. Synthesis of N1′-([^{11}C]methyl)-naltrindole ([^{11}C]MeNTI): a radioligand for positron emission tomographic studies of delta opioid receptors. *J. Label. Compd. Radiopharm.* **1995**, *36*, 137−145. (b) Lever, J. R.; Scheffel, U.; Kinter, C. M.; Ravert, H. T.; Dannals, R. F.; Wagner, H. N., Jr.; Frost, J. J. In vivo binding of N1′-([^{11}C]methyl) naltrindole to δ-opioid receptors in mouse brain. *Eur. J. Pharmacol.* **1992**, *216*, 459−460.

(3) (a) Madar, I.; Lever, J. R.; Kinter, C. M.; Scheffel, U.; Ravert, H. T.; Musachio, J. L.; Mathews, W. B.; Dannals, R. F.; Frost, J. J. Imaging δ opioid receptors in human brain by N1′-([^{11}C]methyl)-naltrindole and PET. *Synapse* **1996**, *24*, 19−28. (b) Smith, J. S.; Zubieta, J.-K.; Price, J. C.; Flesher, J. E.; Madar, I.; Lever, J. R.; Kinter, C. M.; Dannals, R. F.; Frost, J. J. Quantification of δ-opioid receptors in human brain with *N*1′-([^{11}C]methyl)naltrindole and positron emission tomography. *J. Cereb. Blood Flow Metab.* **1999**, *19*, 956−966.

(4) Madar, I.; Lesser, R. P.; Krauss, G.; Zubieta, J.-K.; Lever, J. R.; Kinter, C. M.; Ravert, H. T.; Musachio, J. L.; Mathews, W. B.; Dannals, R. F.; Frost, J. J. Imaging of delta- and mu-opioid receptors in temporal lobe epilepsy by positron emission tomography. *Ann. Neurol.* **1997**, *41*, 358−367.

(5) Portoghese, P. S.; Sultana, M.; Takemori, A. E. Design of peptidomimetic δ opioid receptor antagonists using the message-address concept. *J. Med. Chem.* **1990**, *33*, 1714−1720.

(6) (a) Mathews, W. B.; Kinter, C. M.; Palmer, J.; Daniels, R. V.; Ravert, H. T.; Dannals, R. F.; Lever, J. R. Synthesis of *N*1′-([^{18}F]fluoroethyl)-naltrindole ([^{18}F]FEtNTI): a radioligand for positron emission tomographic studies of delta opioid receptors. *J. Label. Compd. Radiopharm.* **1999**, *42*, 43−54. (b) Clayson, J.; Jales, A.; Tyacke, R. J.; Hudson, A. L.; Nutt, D. J.; Lewis, J. W.; Husbands, S. M. Selective δ-opioid receptor ligands: potential PET ligands based on naltrindole. *Bioorg. Med. Chem. Lett.* **2001**, *11*, 939−943.

(7) Akgun, E.; Sajjad, M.; Portoghese, P. S. *N*1′-(*p*-[^{18}F]fluorobenzyl) naltrindole (*p*-[^{18}F]BNTI): a potential PET imaging agent for DOP receptors. *J. Label. Compd. Radiopharm.* **2006**, *49*, 857−866.

(8) Lever, J. R.; Mathews, W. B.; Allmon, R. L.; Kinter, C. M.; Rauseo, P. A.; Scheffel, U. Synthesis and binding studies of ligands selective for delta opioid receptors: radioiodinated (*E*)- and (*Z*)- *N*1′-(3-iodoallyl)naltrindole. *J. Label. Compd. Radiopharm.* **2003**, *46*, S36.

(9) Korlipara, V.; Ells, J.; Wang, J.; Tam, S.; Elde, R.; Portoghese, P. Fluorescent *N*-benzylnaltrindole analogues as potential delta opioid receptor selective probes. *Eur. J. Med. Chem.* **1997**, *32*, 171−174.

(10) Waterhouse, R. N. Determination of lipophilicity and its use as a predictor of blood−brain barrier penetration of molecular imaging agents. *Mol. Imaging Biol.* **2003**, *5*, 376−389.

(11) (a) Campa, M. J.; Schreiber, G.; Bepler, G.; Bishop, M. J.; McNutt, R. W.; Chang, K. J.; Patz, E. F. Characterization of delta opioid receptors in lung cancer using a novel nonpeptidic ligand. *Cancer Res.* **1996**, *56*, 1695−1701. (b) Schreiber, G.; Campa, M. J.;

Prabhakar, S.; O'Briant, K.; Bepler, G.; Patz, E. F., Jr. Molecular characterization of the human delta opioid receptor in lung cancer. *Anticancer Res.* **1998**, *18*, 1787−1792. (c) Tegeder, I.; Geisslinger, G. Opioids as modulators of cell death and survival - unraveling mechanisms and revealing new indications. *Pharmacol. Rev.* **2004**, *56*, 351−369. (d) Fichna, J.; Janecka, A. Opioid peptides in cancer. *Cancer Metastasis Rev.* **2004**, *23*, 351−366.

(12) (a) Peart, J. N.; Gross, E. R.; Gross, G. J. Opioid-induced preconditioning: recent advances and future perspectives. *Vasc. Pharmacol.* **2005**, *42*, 211−218. (b) Lendeckel, U.; Muller, C.; Rocken, C.; Laube, B.; Tager, M.; Huth, C.; Klein, H. U.; Goette, A. Expression of opioid receptor subtypes and their ligands in fibrillating human atria. *Pacing Clin. Electrophysiol.* **2005**, *28*, S275−S279. (c) Watson, M. J.; Holt, J. D.; O'Neill, S. J.; Wei, K.; Pendergast, W.; Gross, G. J.; Gengo, P. J.; Chang, K. J. ARD-353 [4-((2*R*,5*S*)-4-(*R*)-(4-diethylcarbamoylphenyl)(3-hydroxyphenyl) methyl)-2,5-dimethylpiperazin-1-ylmethyl)benzoic acid], a novel nonpeptide δ receptor agonist, reduces myocardial infarct size without central effects. *J. Pharmacol. Exp. Ther.* **2006**, *316*, 423−430.

(13) (a) Mehendale, S. R.; Yuana, C.-S. Opioid-induced gastrointestinal dysfunction. *Dig. Dis.* **2006**, *24*, 105−112. (b) Philippe, D.; Chakass, D.; Thuru, X.; Zerbib, P.; Tsicopoulos, A.; Geboes, K.; Bulois, P.; Breisse, M.; Vorng, H.; Gay, J.; Colombel, J.-F.; Desreumaux, P.; Chamaillard, M. Mu opioid receptor expression is increased in inflammatory bowel diseases: implications for homeostatic intestinal inflammation. *Gut* **2006**, *55*, 815−823. (c) Pol, O.; Palacio, J. R.; Puig, M. M. The expression of δ- and κ-opioid receptor is enhanced during intestinal inflammation in mice. *J. Pharmacol. Exp. Ther.* **2003**, *306*, 455−462.

(14) (a) Stein, C.; Schäfer, M.; Machelska, H. Attacking pain at its source: new perspectives on opioids. *Nat. Med.* **2003**, *9*, 1003−1008. (b) Eisenach, J. C.; Carpenter, R.; Curry, R. Analgesia from a peripherally active κ-opioid receptor agonist in patients with chronic pancreatitis. *Pain* **2003**, *101*, 89−95.

(15) Villemagne, P. S. R.; Dannals, R. F.; Ravert, H. T.; Frost, J. J. PET imaging of human cardiac opioid receptors. *Eur. J. Nucl. Med. Mol. Imaging* **2002**, *29*, 1385−1388.

(16) Madar, I.; Bencherif, B.; Lever, J.; Heitmiller, R. F.; Yang, S. C.; Brock, M.; Brahmer, J.; Ravert, H.; Dannals, R.; Frost, J. J. Imaging δ- and μ-opioid receptors by PET in lung carcinoma patients. *J. Nucl. Med.* **2007**, *48*, 207−213.

(17) Villemagne, P. M.; Bluemke, D. A.; Dannals, R. F.; Ravert, H. T.; Frost, J. J. Imaging opioid receptors in human breast cancer by PET. *J. Nucl. Med.* **2002**, *43S*, 280P.

(18) (a) Lever, S. Z.; Lydon, J. D.; Cutler, C. S.; Jurisson, S. S. Radioactive Metals in Imaging and Therapy. In *Comprehensive Coordination Chemistry II*; McCleverty, J. A., Meyer, T. J., Eds.; Vol. 9, Chapter 20, Ward, M. D. Ed.; Elsevier Science: Oxford, U.K., 2003; pp 883−911. (b) Anderson, C. J.; Welch, M. J. Radiometal-labeled agents (non-technetium) for diagnostic imaging. *Chem. Rev.* **1999**, *99*, 2219−2234.

(19) (a) Jurisson, S. S.; Lydon, J. D. Potential technetium small molecule radiopharmaceuticals. *Chem. Rev.* **1999**, *99*, 2205−2218. (b) Schibli, R.; Schubiger, P. A. Current use and future potential of organometallic radiopharmaceuticals. *Eur. J. Nucl. Med. Mol. Imaging* **2002**, *29*, 1529−1542. (c) Storr, T.; Thompson, K. H.; Orvig, C. Design of targeting ligands in medicinal inorganic chemistry. *Chem. Soc. Rev.* **2006**, *35*, 534−544. (d) Liang, F.; Wan, S.; Li, Z.; Xiong, X.; Yang, L.; Zhou, X.; Wu, C. Medical applications of macrocyclic polyamines. *Curr. Med. Chem.* **2006**, *13*, 711−727.

(20) A preliminary account of one aspect of this work has appeared: Lever, J. R.; Duval, R. A.; Allmon, R. L.; Carmack, T. L.; Watkinson, L. D. Synthesis and pharmacological studies of an indium-labeled DOTA conjugate of naltrindole having high affinity for delta opioid receptors. In *Technetium, Rhenium and other Metals in Chemistry and Nuclear Medicine*, 7th ed.; Mazzi, U., Ed.; SGE Editoriali: Padova, Italy, 2006; pp 207−210.

(21) Keire, D. A.; Jang, Y.-H.; Li, L.; Dasgupta, S.; Goddard, W. A., III; Shively, J. E. Chelators for radioimmunotherapy: I. NMR and ab initio calculation studies on 1,4,7,10-tetra(carboxyethyl)-1,4,7,10-tetraazacyclododecane (DO4Pr) and 1,4,7-tris(carboxymethyl)-10-(carboxyethyl)-1,4,7,10-tetraazacyclododeca ne (DO3A1Pr). *Inorg. Chem.* **2001**, *40*, 4310−4318.

(22) Abdel-Magid, A. F.; Carson, K. G.; Harris, B. D.; Maryanoff, C. A.; Shah, R. D. Reductive amination of aldehydes and ketones with sodium triacetoxyborohydride. Studies on direct and indirect reductive amination procedures. *J. Org. Chem.* **1996**, *61*, 3849−3862.

(23) Liu, S.; He, Z.; Hsieh, W.-Y.; Fanwick, P. E. Synthesis, characterization, and X-ray crystal structure of In(DOTA-AA) (AA = *p*-aminoanilide): A Model for ^{111}In-labeled DOTA-biomolecule conjugates. *Inorg. Chem.* **2003**, *42*, 8831 − 8837.

(24) Hansch, C. A quantitative approach to biochemical structure-activity relationships. *Acc. Chem. Res.* **1969**, *2*, 232−239.

(25) Noy, N.; Zakim, D. Physical-chemical basis for the uptake of organic compounds by cells. In *Hepatic Transport and Bile Secretion: Physiology and Pathophysiology*; Tavoloni, N., Berk, P. D., Eds.; Raven Press: New York, 1993; pp 313−335.

(26) (a) Fang, L.; Knapp, R. J.; Horvath, R.; Matsunaga, T. O.; Haaseth, R. C.; Hruby, V. J.; Porreca, F.; Yamamura, H. I. Characterization of [^{3}H]naltrindole binding to delta opioid receptors in mouse brain and mouse vas deferens: evidence for delta opioid receptor heterogeneity. *J. Pharmacol. Exp. Ther.* **1994**, *268*, 836−846. (b) Contreras, P. C.; Tam, L.; Drower, E.; Rafferty, M. F. [^{3}H]naltrindole: a potent and selective ligand for labeling δ-opioid receptors. *Brain Res.* **1993**, *604*, 160−164.

(27) Heyl, D. L.; Mosberg, H. I. Substitution on the Phe^3 aromatic ring in cyclic δ opioid receptor selective dermorphind/deltorphin tetrapeptide analogues: electronic and lipophilic requirements for receptor affinity. *J. Med. Chem.* **1992**, *35*, 1535−1541.

(28) Coop, A.; Rothman, R. B.; Dersch, C.; Partilla, J.; Porreca, F.; Davis, P.; Jacobson, A. E.; Rice. K. C. δ Opioid affinity and selectivity of 4-hydroxy-3-methoxyindolomorphinan analogues related to naltrindole. *J. Med. Chem.* **1999**, *42*, 1673−1679.

(29) Casy, A. F.; Parfitt, R. T. *Opioid Analgesics, Chemistry and Receptors*; Plenum Press: New York, 1986; pp 470−472.

(30) (a) Kane, B. E.; Svensson, B.; Ferguson, D. M. Molecular recognition of opioid receptor ligands. *AAPS J.* **2006**, *8*, E126−137. (b) Valiquette, M.; Vu, H. K.; Yue, S. Y.; Wahlestedt, C.; Walker, P. Involvement of Trp-284, Val-296, and Val-297 of the human δ-opioid receptor in binding of δ-selective ligands. *J. Biol. Chem.* **1996**, *271*, 18789−18796. (c) Metzger, T. G.; Paterlini, M. G.; Ferguson, D. M.; Portoghese, P. S. Investigation of the selectivity of oxymorphone- and naltrexone-derived ligands via site-directed mutagenesis of opioid receptors: exploring the 'address' recognition locus. *J. Med. Chem.* **2001**, *44*, 857−862.

(31) Lever, J. R.; Gustafson, J. L.; Xu, R.; Allmon, R. L.; Lever, S. Z. σ1 and σ2 receptor binding affinity and selectivity of SA4503 and fluoroethyl SA4503. *Synapse* **2006**, *59*, 350−358.

(32) Kenakin, T. *Pharmacologic Analysis of Drug-Receptor Interaction*, 2nd ed.; Raven Press: New York, 1993; pp 137−175.

(33) (a) Chivers, J. K.; Gommeren, W.; Leysen, J. E.; Jenner, P.; Marsden, C. D. Comparison of the in-vitro receptor selectivity of substituted benzamide drugs for brain neurotransmitter receptors. *J. Pharm. Pharmacol.* **1987**, *40*, 415−421. (b) Blin, O. A comparative review of new antipsychotics. *Can. J. Psychiatry* **1999**, *44*, 235−244.

(34) Dupin, S.; Tafani, J.; Mazarguil, H.; Zajac, J. [^{125}I][D-Ala^2]Deltorphin-I: a high affinity, delta-selective opioid receptor ligand. *Peptides* **1991**, *12*, 825−830.

(35) Drower, E. J.; Dorn, C. R.; Markos, C. S.; Unnerstall, J. R.; Rafferty, M. F.; Contreras, P. C. Quantitative light microscopic localization of [^{3}H]naltrindole binding sites in the rat brain. *Brain Res.* **1993**, *602*, 138−142.

(36) Zimlichman, R.; Gefel, D.; Eliahou, H.; Matas, Z.; Rosen, B.; Gass, S.; Ela, C.; Eilam, Y.; Vogel, Z.; Barg, J. Expression of opioid receptors during heart ontogeny in normotensive and hypertensive rats. *Circulation* **1996**, *93*, 1020−1025.

(37) Khawaja, X. Z.; Green, I. C.; Thorpe, J. R.; Titheradge, M. A. The occurrence and receptor specificity of endogenous opioid peptides within the pancreas and liver of the rat. Comparison with brain. *Biochem. J.* **1990**, *267*, 233−240.

(38) Boyadjieva, N. I.; Chaturvedi, K.; Poplawski, M. M.; Sarkar, D. K. Opioid antagonist naltrexone disrupts feedback interaction between μ and δ opioid receptors in splenocytes to prevent alcohol inhibition of NK cell function. *J. Immunol.* **2004**, *173*, 42−49.

(39) (a) Nishimura, E.; Buchan, A. M,; McIntosh, C. H. Autoradiographic localization of opioid receptors in the rat stomach. *Neurosci. Lett.* **1984**, *50*, 73−78. (b) Nishimura, E.; Buchan, A. M.; McIntosh, C. H. Autoradiographic localization of μ- and δ-type opioid receptors in the gastrointestinal tract of the rat and guinea pig. *Gastroenterology* **1986**, *91*, 1084−1094. (c) De Luca, A.; Coupar, I. M. Insights into opioid action in the intestinal tract. *Pharmacol. Ther.* **1996**, *69*, 103−115. (d) Townsend, D., IV; Brown, D. R. Predominance of δ-opioid-binding sites in the porcine enteric nervous system. *J. Pharmacol. Exp. Ther.* **2002**, *300*, 900−909.

(40) Evans, A. A.; Tunnicliffe, G.; Knights, P.; Bailey, C. J.; Smith, M. E. Delta opioid receptors mediate glucose uptake in skeletal muscles of lean and obese-diabetic (ob/ob) mice. *Metabolism* **2001**, *50*, 1402−1408.

(41) Oude Elferink, R. P. J.; Meijer, D. K. F.; Kuipers, F.; Jansen, P. L. M.; Groen, A. K.; Groothuis, G. M. M. Hepatobiliary secretion of organic compounds; molecular mechanisms of membrane transport. *Biochim. Biophys. Acta.* **1995**, *1241*, 215−268.

(42) Rivory, L. P.; Avent, K. M.; Pond, S. M. Effects of lipophilicity and protein binding on the hepatocellular uptake and hepatic disposition of two anthracyclines, doxorubicin and iododoxorubicin. *Cancer Chemother. Pharmacol.* **1996**, *38*, 439−445.

(43) Bhargava, H. N.; Villar, V. M.; Cortijo, J.; Morcillo, E. J. Binding of [^{3}H][D-Ala^2, MePhe^4, Gly-ol^5] enkephalin, [^{3}H][D-Pen^2, D-Pen5]-enkephalin, and [^{3}H]U-69,593 to airway and pulmonary tissues of normal and sensitized rats. *Peptides* **1997**, *18*, 1603−1608.
(44) Mercadante, S; Arcuri, E. Opioids and renal function. *J. Pain* **2004**, *5*, 2−19.
(45) Sezen, S. F.; Kenigs, V. A.; Kapusta, D. R. Renal excretory responses produced by the delta opioid agonist, BW373U86, in conscious rats. *J. Pharmacol. Exp. Ther.* **1998**, *287*, 238−245.
(46) Wittert, G.; Hope, P.; Pyle, D. Tissue distribution of opioid receptor gene expression in the rat. *Biochem. Biophys. Res. Commun.* **1996**, *218*, 877−881.
(47) Bidlack, J. M. Detection and function of opioid receptors on cells from the immune system. *Clin. Diagn. Lab. Immunol.* **2000**, *7*, 719−723.
(48) Weber, S. J.; Greene, D. L.; Hruby, V. J.; Yamamura, H. I.; Porreca, F.; Davis, T. P. Whole body and brain distribution of [^{3}H]cyclic [D-Pen^2, D-Pen^5] enkephalin after intraperitoneal, intravenous, oral and subcutaneous administration. *J. Pharmacol. Exp. Ther.* **1992**, *263*, 1308−1316.
(49) Collier, T. L.; Schiller, P. W.; Waterhouse, R. N. Radiosynthesis and in vivo evaluation of the pseudopeptide δ-opioid antagonist [^{125}I]-ITIPP(ψ). *Nucl. Med. Biol.* **2001**, *28*, 375−381.
(50) Lever, J. R.; Watson, T. A.; Owen, N. K.; Fitzsimmons, J. M.; Mazuru, D. G.; Hoffman, T. J. In vivo localization of opioid receptors on human breast cancer xenografts in SCID mice. *J. Nucl. Med.* **2002**, *43S*, 282P.

JM0700013